Methylglyoxal-derived glycated albumin enhances the stemness potential of invasive ductal carcinoma-derived breast cancer stem-like cell line KAIMRC1

MARAM ALDAWOOD[1,2], MARIAM K. ALAMOUDI[3], ABDULMONEM A. ALSALEH[2,4], NOUF ALHARBI[5], SARAH HUWAIZI[6], REHAB ALROSHODY[2], RIZWAN ALI[4,5], RAFA ALMEER[1] and SABINE MATOU-NASRI[2,4,7]

[1]Zoology Department, King Saud University, Riyadh 11451, Saudi Arabia; [2]Blood and Cancer Research Department, King Abdullah International Medical Research Center, Riyadh 11481, Saudi Arabia; [3]Department of Pharmacology, College of Pharmacy, Prince Sattam Bin Abdulaziz University, Al-Kharj 11942, Saudi Arabia; [4]King Saud bin Abdulaziz University for Health Sciences, Riyadh 11481, Saudi Arabia; [5]Medical Genomics Research Department, King Abdullah International Medical Research Center, Riyadh 11481, Saudi Arabia; [6]Medical Research Core Facility and Platforms, King Abdullah International Medical Research Center, Riyadh 11481, Saudi Arabia; [7]Biosciences Department, Faculty of the School for Systems Biology, George Mason University, Manassas, VA 22030, USA

Received October 03, 2025; Accepted February 19, 2026

DOI: 10.3892/ol.2026.15541

Abstract. Type 2 diabetes mellitus (T2DM) is a risk factor for breast cancer (BC) development and recurrence due to multifactorial mechanisms, including the generation of glycated proteins under hyperglycemic conditions. Emerging evidence indicates that hyperglycemia promotes the formation and expansion of BC stem-like cells (BCSC), contributing to worse outcomes in patients with T2DM. To support early detection and personalized therapy, there is an urgent need to identify novel biomarkers that specifically target BCSCs in patients with T2DM. The present study examined the effects of glycated albumin (GA) on the cellular functions of KAIMRC1, a naturally immortalized BCSC line derived from invasive ductal carcinoma (IDC), the primary breast carcinoma developed in patients with T2DM. Cells were subjected to *in vitro* assays, including soft agar colony formation, real-time monitoring of cell proliferation, motility and invasion through a reconstituted basement membrane using the xCELLigence system and western blotting. A triple-negative BC cell line was used as a comparator. Aldehyde dehydrogenase (ALDH) activity was quantified using a biochemical assay. As expected, KAIMRC1 cells exhibited high ALDH activity, a characteristic feature of cancer stem-like cells (CSCs). GA induced dose-dependent increases in KAIMRC1 cell proliferation, motility, invasion and colony formation and was associated with elevated levels of the oncoprotein phosphorylated-ERK1/2, the receptor for advanced glycation end products (RAGE) and the stemness-associated proteins OCT3/4 and vimentin. GA-treated KAIMRC1 cells showed notable invasive capacity despite slow proliferation, consistent with known metastatic potential of quiescent CSCs. Conversely, unglycated albumin had no detectable biological effects except for an anti-mitogenic response at high concentration. Bioinformatics analyses showed that vimentin mRNA was upregulated in patients with BC and DM and was associated with a poor prognosis in patients with BC. RAGE neutralization attenuated GA-induced vimentin upregulation. Altogether, these findings show that GA exerts pro-tumorigenic effects in IDC-derived CSCs and upregulates vimentin protein expression via RAGE, highlighting the GA-RAGE axis as a potential therapeutic target

Correspondence to: Dr Sabine Matou-Nasri, Blood and Cancer Research Department, King Abdullah International Medical Research Center, Riyadh 11481, Saudi Arabia
E-mail: matouepnasrisa@mngha.med.sa

Abbreviations: AGEs, advanced glycation end products; ALDH, aldehyde dehydrogenase; BC, breast cancer; BSA, bovine serum albumin; CIM, cellular invasion/migration; CPM, counts per million; CSC, cancer stem-like cells; DM, diabetes mellitus; DMEM, Dulbecco's modified Eagle's medium; EMT, epithelial-mesenchymal transition; ERK, extracellular signal-regulated kinase; GA, glycated albumin; GAPDH, glyceraldehyde 3-phosphate dehydrogenase; IDC, invasive ductal carcinoma; IgG, immunoglobulin G; IGF, insulin-like growth factor; LSM, low-serum medium; METABRIC, molecular taxonomy of breast cancer international consortium; MG, methylglyoxal; NAD, nicotinamide adenine dinucleotide; OCT, octamer-binding transcription factor; p, phosphorylated; PAM, PI3K/Akt/mTOR; PAM50, prediction analysis of microarray 50; RAGE, receptor for advanced glycation end products; RT, room temperature; RTCA-DP, Real-time Cell Analyzer Dual Purpose; SCAN-B, Swedish Cancerome Analysis Network-Breast; T1DM, type 1 diabetes mellitus; T2DM, type 2 diabetes mellitus; TBS, Tris-buffered saline; TMM, Trimmed Mean of M-values; TNBC, triple-negative breast cancer

Key words: triple-negative breast cancer, invasive ductal carcinoma, cancer stem-like cells, type 2 diabetes mellitus, glycated albumin, vimentin

and supporting vimentin as a promising prognostic marker for invasive BC in patients with DM.

Introduction

Diabetes mellitus (DM) is a chronic metabolic disorder characterized by elevated blood glucose (hyperglycemia), insulin (hyperinsulinemia) and lipids (hyperlipidemia), and it represents a growing global health challenge (1). According to the International Diabetes Federation, in 2024, >589 million individuals aged 20-79 years were diagnosed with DM, and this number is projected to increase to 853 million by 2050, predominantly affecting populations in low- and middle-income countries (2,3). DM is classified into different types, including type 1 DM (T1DM), which is primarily driven by genetic defects leading to autoimmune destructions of pancreatic insulin-producing cells (4). Type 2 DM (T2DM) arises from dysregulated protein, carbohydrate and lipid metabolism due to insulin resistance, impaired insulin secretion or a combination of both (5). Mainly influenced by environmental factors such as diet, lack of exercise and aging, T2DM is notably more prevalent when compared with gestational diabetes or T1DM, accounting for 90-95% of all cases of diabetes (3). The economic and clinical burden of DM is substantial, as patients frequently experience complications, including vascular malformations, cardiovascular diseases, neurodegenerative disorders and various types of cancer, despite treatment with antidiabetic agents such as metformin, a glucagon-like peptide-1 receptor agonist (5-9). These observations underscore the urgent need for early screening and the development of therapeutic strategies for patients with DM who have an increased risk of developing cancer, often diagnosed at an advanced and clinically challenging stage due to drug resistance (10-12).

Numerous epidemiological studies indicate that T2DM is associated with an increased risk for several types of cancer, particularly breast cancer (BC), including early-stage non-metastatic BC and a 20-30% higher risk of invasive BC compared with non-diabetic individuals (13-16). BC is the most frequently diagnosed cancer in women worldwide, with >2.3 million new cases and 665,000 mortalities reported in 2022 (17). The impact of T2DM on BC, particularly invasive BC, has been estimated to increase both incidence and mortality by ~20%, primarily due to poor glycemic control, delayed diagnosis, advanced disease stage, poor prognosis and limited efficacy of systemic anticancer treatments such as chemotherapy and immunotherapy (18-20). Furthermore, specific cancer therapies induce insulin resistance in patients with BC, contributing to T2DM development and underscoring shared and overlapping pathophysiological mechanisms between the two conditions (21,22). Advanced glycation end products (AGEs) abundantly generated through non-enzymatic glycation under hyperglycemic conditions, and insulin-like growth factors (IGFs), overproduced during hyperinsulinemia, contribute to tumorigenesis through multiple mechanisms (23,24). In addition to inducing oxidative stress and inflammation, both AGEs and IGFs activate oncogenic signaling pathways, including RAS/MAPK, PI3K/Akt/mTOR (PAM), NF-κB and JAK/STAT pathways, through their respective receptors, receptor for AGEs (RAGE) and IGF receptors, thereby stimulating tumor development and progression via metastasis (25,26).

BC stem-like cells (BCSCs) have been identified in invasive ductal carcinoma (IDC), which originates in milk ducts and accounts for 80% of invasive cases of BC (27,28). Generally, cancer stem-like cells (CSCs) are characterized by their capacity for self-renewal, differentiation, motility, metastasis and resistance to anticancer therapies, traits that contribute to tumor aggressiveness and progression (29,30). In various BC subtypes, these small cell populations, representing ~2% of tumor tissue, express a range of stemness markers, such as $CD44^+/CD24^-$, high aldehyde dehydrogenase (ALDH) activity, octamer-binding transcription factor (OCT)3/4 and vimentin expression (31,32).

In the present study, a naturally immortalized cell line, KAIMRC1, derived from IDC tissue obtained from a Saudi female patient established by Ali *et al* (33) was used. KAIMRC1 was characterized as a stem-like based on the expression of canonical stem cell markers, including $CD44^+/CD24^-$, and its tumorigenicity was confirmed through spheroid formation in soft agar (33). Hyperglycemia promotes CSC generation by creating a tumor environment that supports its expansion, tumorigenicity and aggressiveness (34,35). Clinical observations have reported elevated glycated albumin (GA) levels in blood collected from individuals with DM (36,37). The pro-oncogenic effects of GA on triple-negative BC (TNBC) and estrogen receptor-positive BC cell lines have been previously reported (38,39); however, the biological impact of GA on the stemness characteristics of IDC-derived CSCs remains poorly understood. Therefore, in the present study, the tumorigenic response of the IDC-derived BCSC line KAIMRC1 to GA at the cellular and molecular levels was examined, including cell surface and signaling proteins, to identify potential biomarkers for the precise detection of IDC-derived stem-like cells and the development of tailored therapeutic strategies. Bioinformatics analyses were conducted to determine the expression levels of stemness-associated proteins of interest in patients with invasive BC and DM and to evaluate their impact on overall survival.

Materials and methods

Reagents. Mouse primary monoclonal antibodies directed against extracellular signal-regulated kinase (ERK)1 (clone G-8; cat. no. sc-271269), phosphorylated-ERK1/2 (p-ERK1/2; clone E-4; Tyr204 of ERK1; cat. no. sc-7383), OCT3/4 (clone A-9; cat. no. sc-365509) and RAGE (clone E-1; cat. no. sc-74473) were obtained from Santa Cruz Biotechnology, Inc. Mouse monoclonal antibodies targeting vimentin (V9; cat. no. 790-2917) and glyceraldehyde 3-phosphate dehydrogenase (GAPDH; clone 6C5; cat. no. ab8245) were sourced from Roche Diagnostics GmbH and Abcam, respectively. Mouse monoclonal anti-RAGE antibody (clone 02; cat. no. MA5-29007) and isotype control immunoglobulin (IgG; cat. no. 31235) were purchased from Invitrogen, Thermo Fisher Scientific, Inc. The secondary antibodies, IRDye 680RD (red)-conjugated goat anti-rabbit (cat. no. 926-68071) and IRDye 800RD (green)-conjugated goat anti-mouse (cat. no. 926-32210) were provided by LI-COR Biosciences. All other reagents were obtained from Thermo Fisher Scientific, Inc. unless otherwise specified.

Preparation of GA and unglycated albumin. GA was generated as previously described (38-40). Briefly, bovine serum albumin (BSA; fraction V; 10 mg/ml) was incubated with 0.1 M methylglyoxal (MG) in 0.1 M sodium phosphate buffer (pH 7.4) containing 3 mM sodium azide for 72 h at 37˚C to induce glycation. Unglycated albumin was processed using the same procedure but without MG. Free MG (unbound sugar) was removed by dialysis against distilled water, using a Slide-A-lyzer® mini dialysis device with a molecular weight cutoff of 3.5 kDa (cat. no. 69550). Endotoxin levels were negligible after purification with Detoxi-gel endotoxin-removing gel columns (cat. no. 20344) and assessment with the E-TOXATE kit (cat. no. ET0200; MilliporeSigma), according to the manufacturers' instructions. As shown in Fig. S1, GA formation was characterized and confirmed by the increase in fluorescence intensity measured using a SpectraMax M5 fluorescence spectrophotometer (Molecular Devices, LLC). Protein concentrations were determined using the Qubit™ protein assay (cat. no. Q33211) on the Invitrogen Qubit 3 fluorometer. To ensure the stability of the GA and unglycated BSA solutions, aliquots were prepared and stored at -20˚C until use.

Culture and treatment of IDC-derived KAIMRC1 stem-like cells and TNBC cell line MDA-MB-231. The IDC-derived KAIMRC1 stem-like cell line (Resource Identification Initiative: CVCL_RW19), classified as $ER^+/HER2^-$ subtype exhibiting stemness features, was cultured in a complete medium consisting of advanced Dulbecco's modified eagle (DMEM) supplemented with 10% heat-inactivated fetal bovine serum (FBS), 2 mM glutamine and antibiotics (100 IU/ml penicillin; 100 μg/ml streptomycin) (33). Cultures were maintained at 37˚C in a humidified incubator containing 5% CO_2. The TNBC cell line MDA-MB-231 (cat. no. HTB-26, American Type Culture Collection) was maintained in complete DMEM supplemented with the aforementioned components. At confluence, MDA-MB-231 cells were passaged every 2-3 days using enzymatic digestion with TrypLE™ Express Enzyme solution, whereas KAIMRC1 stem-like cells were easily detached from the culture flasks. Both cell lines were subcultured at a ratio of 1:2 or 1:3. For treatment, cells were exposed to GA and unglycated BSA at concentrations of 25, 50, 100 and 200 μg/ml in low-serum medium (LSM), consisting of low glucose (1 g/l) DMEM supplemented with 2.5% FBS, for designated incubation periods. Untreated cells served as controls.

ALDH activity assay. The nicotinamide adenine dinucleotide (NAD)-dependent ALDH activity colorimetric assay (cat. no. ab155893; Abcam) was performed according to the manufacturer's instructions. Briefly, a reduced NAD (NADH) standard curve was generated by preparing 0, 2, 4, 6, 8 and 10 nmol/well NADH standards corresponding to 0, 2, 4, 6, 8 and 10 μl NADH solutions dispensed in duplicate into a 96-well plate. The final volume for each standard was adjusted to 50 μl/well using an ALDH assay buffer. Untreated cells ($1x10^6$) were homogenized in 200 μl ice-cold assay buffer for 10 min and centrifuged at 12,000 x g for 5 min at 4˚C and 50 μl of the resulting supernatant was transferred to a 96-well plate and mixed with 50 μl assay buffer. Subsequently, 50 μl reaction mix was added to each well, and the plate was incubated at room temperature (RT) for 5 min. Optical density was recorded at 450 nm for the samples and their corresponding backgrounds controls at the initial time points (A_1 and A_{1B}), and again after 60 min (A_2 and A_{2B}). ALDH activity (mU/ml) was calculated using the following equation:

$$\text{ALDH activity} = B/\{[(A_2-A_{2B})-(A_1-A_{1B})] \times V \times \text{dilution factor}\}$$

where B, represents the amount of NADH generated, and V represents the sample volume.

Monitoring real-time cell proliferation, directional motility and invasion using the xCELLigence system. The tumorigenic effects of GA on real-time cell proliferation, directional motility and invasion were assessed using the xCELLigence Real-time Cell Analyzer Dual Purpose (RTCA-DP) system (Agilent Technologies, Inc.) following the manufacturer's instructions. This label-free, impedance-based platform continuously monitors cellular adhesion, growth and motility by measuring changes in electrical impedance across plates incorporating microelectrodes, thus providing a dynamic and quantitative assessment of cell behavior. For cell proliferation, 16-well E-plates were used (cat. no. 0-060-0890; Agilent Technologies, Inc.) and for cell invasion and motility, 16-well cellular invasion/motility (CIM)-plates (cat. no. 05-665-817-001; Agilent Technologies, Inc.) were used for cell proliferation and motility/invasion, respectively. For the cell proliferation assay, 7,500 cells were seeded per well in the E-plate, which was then inserted into RTCA-DP station. A total of 6 h after seeding the TNBC MDA-MB-231 cells and 24 h after seeding the IDC-derived KAIMRC1 stem-like cells, 100 μl complete medium was replaced with 100 ml LSM containing different concentrations (25, 50, 100 and 200 μg/ml) GA and unglycated BSA. The E-plate was then reinserted into the RTCA-DP station. For the cell motility assay, the CIM-16 plate, consisting of an upper and lower chamber, was prepared by hydrating the upper membrane with serum-free medium and filling the lower chamber membrane with LSM containing effective concentrations 50 and 100 μg/ml GA, which served as a chemoattractant. After the prescribed incubation period and before cell seeding, the CIM-16 plates were placed on the RTCA-DP station, and a baseline impedance measurement was obtained using a cell-free medium. Cells (15,000) were then seeded into each well of the upper chamber. The CIM-16 plates were subsequently returned to the RTCA-DP station, and directional cell motility was quantified based on the electrical impedance changes detected as cells migrated through the membrane. The same experimental approach was applied to assess cell invasion, defined as a motility across a reconstituted basement membrane, using the xCELLigence system and CIM-16 plate, except that the upper chamber was first coated with Geltrex™ LDEV-free, reduced-growth factor basement membrane matrix (cat. no. A1413202). Data acquisition and cell index calculations were performed using RTCA software 1.2.1 (cat. no. 30-060-0890; Agilent Technologies, Inc.), and cell index curves were monitored every 15 min for 72-80 h for cell proliferation and 24 h to assess cell motility and invasion.

Colony formation assays. Soft agar colony formation assay for IDC-derived KAIMRC1 stem-like cells was performed in 24-well plates, each well containing two layers of agarose

(cat. no. 121853; Merck KGaA) in complete medium, as previously described (33). The bottom layer contained 0.6% agarose, while the top layer contained 0.35% agarose. To assess colony formation, IDC-derived KAIMRC1 stem-like cells (20,000/well) were seeded into the top agarose layer. After 2-3 days of incubation at 37˚C, the complete medium was replaced with LSM containing GA at concentrations 50 and 100 μg/ml for 72 h at 37˚C. Following treatment, the cells were incubated for 2-3 weeks, and fresh LSM containing GA (50 and 100 μg/ml) was added twice weekly. Colonies were fixed with 4% paraformaldehyde for 5 min at RT and visualized under an inverted ZEISS microscope, and colonies containing >50 cells were counted manually.

For the TNBC cell line MDA-MB-231, cells were harvested and resuspended in serum-free cell culture medium to a final concentration of $1x10^6$ cells/ml. An appropriate number of cells (3,000-5,000 per well) were seeded into 24-well plates. After 24 h, the culture medium was replaced with LSM containing GA at concentrations of 50 and 100 μg/ml. Following treatment, the plates were incubated at 37˚C in a humidified 5% CO_2 incubator for 1 week, until untreated control cells formed colonies of substantial size (>50 cells per colony). Cells were fixed with 4% paraformaldehyde for 5 min at RT. After removing the fixative, 1 ml of 0.5% crystal violet solution was added to each well and incubated for 2 h at RT. Excess stain was carefully removed by rinsing the plates in distilled water, and the plates were air-dried. Colonies were imaged using a ZEISS microscope, colonies containing >50 cells were counted (41).

Preparation of cell lysates and western blot analysis. IDC-derived KAIMRC1 stem-like cells and TNBC MDA-MB-231 cells ($3x10^5$ cells) were seeded in complete medium in 12-well plates and incubated for 24 h at 37˚C. The medium was subsequently replaced with LSM and incubated for an additional 24 h at 37˚C. Cells were treated with GA and unglycated BSA at concentrations of 25, 50, 100 and 200 μg/ml for the indicated incubation periods (10 min and 48 h). After washing in ice-cold phosphate-buffered saline, proteins were extracted by lysing the cells with NP40 lysis buffer. Cell debris were removed by centrifugation at 20,000 x g for 30 min at 4˚C. Protein concentration for each sample was determined using the Qubit Protein Assay, and total protein amount was adjusted to 100 or 200 μg for equal protein loading. Protein samples were mixed with an equal volume of 4X Laemmli sample buffer in 1.5 ml Eppendorf® tubes, denatured by boiling at 95˚C for 15 min and then briefly centrifuged at 1,000 x g for 7 sec at RT. Samples were resolved on 11% SDS-PAGE gels alongside prestained molecular weight markers. Proteins were then electroblotted onto PVDF membranes, which were blocked for 1 h at RT in Tris-buffered saline (TBS)-0.1% Tween (pH 7.4) containing 1% BSA. PVDF membranes were incubated overnight at 4˚C on a rotating shaker with mouse or rabbit primary antibodies diluted in the blocking buffer, targeting p-ERK1 (1:500 dilution), total ERK1 (1:500 dilution), OCT3/4 (1:500 dilution), RAGE (1:1,000 dilution), vimentin (1:1,000 dilution) and the housekeeping protein GAPDH (1:5,000 dilution). Following five washes for 10 min each in TBS-0.1% Tween at RT, membranes were incubated for 1 h at RT with infrared fluorescent secondary antibodies diluted (1:5,000 dilution) in LI-COR Odyssey® blocking buffer: IRDye 680RD (red)-conjugated goat anti-rabbit or IRDye 800RD (green)-conjugated goat anti-mouse (LI-COR Biosciences) with continuous mixing. After washing, protein bands were visualized using the LI-COR Odyssey CLx Scanner, and protein expression levels were quantified using ImageJ software version 1.53e (https://imagej.net/ij/index.html) as previously described (39,42).

Bioinformatics. The MammOnc-DB database (http://resource.path.uab.edu/MammOnc-Home.html; accessed, 19 September 2025) was used to analyze proteins of interest (43). Gene expression profiles of the genes encoding RAGE (*AGER*), vimentin (*VIM*) and OCT4 (*POU5F1*), were stratified by biopsy type and TNBC status, as well as their associations with 5-year survival in patients with BC, retrieved from the Swedish Cancerome Analysis Network-Breast (SCAN-B) within MammOnc-DB database (43,44). Additional gene expression profiles for these genes, categorized according to three-gene classifier subtypes ($HER2^+$, ER^+HER2^- and ER^-HER2^-), were obtained from the Molecular Taxonomy of Breast Cancer International Consortium (METABRIC) dataset available through MammOnc-DB (43,45). Further analyses were conducted using the cBioPortal database (https://www.cbioportal.org/; accessed, 19 September 2025) (46-48). The dataset 'Breast Cancer (METABRIC, Nature 2012 & Nat Commun 2016)' within the 'breast' section was applied to assess gene expression profiles of the analyzed genes based on prediction analysis of microarray 50 (PAM50) and claudin subtype classifications (45,49,50). Patients were classified into low- and high-expression groups using the median mRNA expression values (Illumina HT-12 v3 microarray; Illumina, Inc.) for each gene. Corresponding clinical data were downloaded from the database.

Data from Panigrahi *et al* (51) was retrieved from the Gene Expression Omnibus data repository (GSE202922; accessed on 23 June 2025). Processed RNA sequencing count data were normalized using counts per million (CPM) after trimmed mean of M-values (TMM) normalization (CPM-TMM) method (51).

RAGE neutralization. RAGE was neutralized in the cells by treating them with an anti-RAGE antibody to determine whether GA exerts its effects through this receptor. IDC-derived KAIMRC1 stem-like and TNBC MDA-MB-231 cells ($3x10^5$ cells) were seeded in complete media as previously described51 a40). After medium replacement with LSM, 20 μg/ml mouse monoclonal anti-RAGE antibody (clone 02; cat. no. MA5-29007) or 20 μg/ml isotype control IgG (cat. no. 31235) was added. Following a 2 h incubation at 37˚C, the cells were stimulated with 100 μg/ml GA for 48 h, which represented the most effective concentration used in earlier experiments of the present study. Protein lysates were then collected for western blot analysis.

Statistical analysis. All data are presented as the mean ± SD from three independent experiments. Statistical comparisons between the two groups were performed using an unpaired two-tailed student's t-test. For analysis involving more than two groups, one-way ANOVA statistical test followed by Tukey's post hoc test was used to assess statistical differences

among multiple comparisons. Statistical outputs for bioinformatics analyses were derived from the SCAN-B and METABRIC datasets within the MammOnc-DB database, as well as the 'Breast Cancer (METABRIC, Nature 2012 & Nat Commun 2016)' dataset accessed through the cBioPortal database. Pairwise comparisons for datasets generated by Panigrahi *et al* (51) were evaluated using the Mann-Whitney U non-parametric test. P<0.05 was considered to indicate a statistically significant difference.

Results

IDC-derived KAIMRC1 stem-like cells exhibit higher ALDH activity when compared with TNBC MDA-MB-231 cells. High ALDH activity is widely recognized as a valuable biomarker for CSCs, particularly BCSCs, because it supports their stemness and self-renewal properties (52). Therefore, ALDH activity was first assessed in IDC-derived KAIMRC1 and TNBC MDA-MB-231 cells to identify the cell line with greater stem-like properties. The KAIMRC1 cell line showed significantly higher ALDH enzyme activity (1.36-fold; P=0.019) compared with the MDA-MB-231 cell line (Fig. 1).

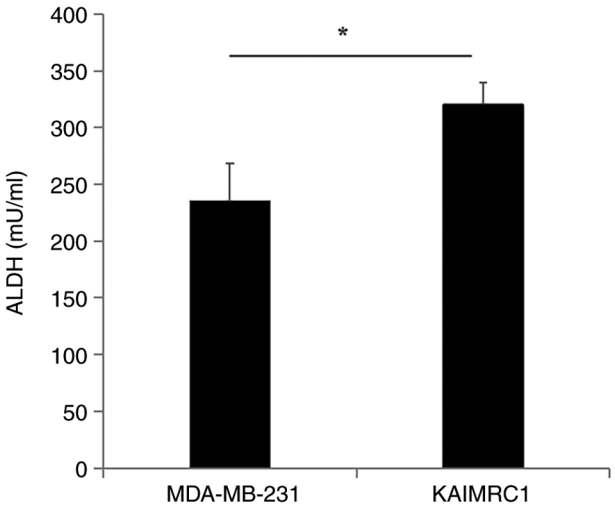

Figure 1. ALDH activity in triple-negative breast cancer MDA-MB-231 and invasive ductal carcinoma-derived KAIMRC1 cells measurements using a colorimetric assay. KAIMRC1 stem-like cells showed higher ALDH activity when compared with that of MDA-MB-231 cells. Data are presented as the mean ± SD from three independent experiments. Statistical significance relative to MDA-MB-231 cells is indicated as *P<0.05. ALDH, aldehyde dehydrogenase.

GA weakly increases the cell proliferation rate of IDC-derived KAIMRC1 stem-like cells, unlike its effect on TNBC MDA-MB-231 cells. Cell proliferation was monitored using the xCELLigence RTCA-DP system to assess the mitogenic response of stem-like cells. Before examining KAIMRC stem-like cells, the effects of various GA concentrations (25-200 μg/ml) and the expected lack of effect of unglycated BSA on the proliferation of TNBC MDA-MB-231 cells (Fig. S2) were verified and confirmed, consistent with findings using the trypan blue exclusion method (38). Thus, using the real-time system on MDA-MB-231 cells, unglycated BSA did not alter cell proliferation at any concentrations tested, except for a significant reduction at 200 μg/ml (0.83-fold; P=0.02; Fig. S2A). Conversely, GA stimulated the cell proliferation rate in a dose-dependent manner that followed a bell-shaped curve characterized by increased proliferation at intermediate doses (1.28-fold at 50 μg/ml; P=0.00009; 1.59-fold at 100 μg/ml; P=0.00024; Fig. S2B), followed by a decreased proliferation at the highest GA dose (0.79-fold at 200 μg/ml; P=0.019; Fig. S2B). This pattern is consistent with previously described activation kinetics of dimeric receptors such as RAGE (38). After validating the biological effect of GA, KAIMRC1 stem-like cells were treated with intermediate doses of 50 and 100 μg/ml of GA and unglycated BSA. Similar to the findings in MDA-MB-231 cells, 100 mg/ml GA significantly increased cell proliferation of KAIMRC1 stem-like cells (1.27-fold; P=0.0076; Fig. 2), although the onset of the KAIMRC1 cell response was observed after 60 h of incubation (Fig. 2) when compared with MDA-MB-231 cell response observed after 10 h of incubation (Fig. S2B). Unglycated BSA did not affect the cell proliferation of KAIMRC1 stem-like cells compared with untreated controls (Fig. 2).

GA has an increased stimulatory effect on the invasiveness of IDC-derived KAIMRC1 stem-like cells when compared with TNBC MDA-MB-231 cells. Cell motility, which drives migration, invasion and metastasis, is a key process in cancer progression (7). To evaluate directional motility and basement membrane invasion, the automated xCELLigence RTCA-DP system was employed. In IDC-derived KAIMRC1 stem-like cells, treatment with effective GA concentrations, at 50 and 100 μg/ml, significantly enhanced motility capacity, with a 2.37-fold (P=0.00003) and 1.44-fold (P=0.0096) increase, respectively, compared with untreated controls (Fig. 3). TNBC MDA-MB-231 cells exhibited a similar response, showing a 2.52-fold (P=0.0096) and 1.6-fold, (P=0.03) increase at the same GA concentrations, respectively (Fig. S3). When motility was assessed through a protein-based matrix to determine invasive capacity, GA significantly enhanced invasion in both cell lines, though to differing extents. IDC-derived KAIMRC1 stem-like cells exhibited a marked increase in invasiveness upon GA treatment, with 3.71-fold (P=0.004) and 5.14-fold (P=0.0005) enhancements at 50 and 100 μg/ml GA, respectively (Fig. 4). Conversely, TNBC MDA-MB-231 cells showed a significant increase in invasion, with 1.42-fold (P=0.009) and 1.47-fold (P=0.04) enhancements at the effective (50-100 μg/ml) GA concentrations compared with the untreated controls, respectively (Fig. S4). These findings indicate that IDC-derived KAIMRC1 stem-like cells are markedly more responsive to GA-induced invasiveness when compared with MDA-MB-231 cells.

GA promotes colony formation in IDC-derived KAIMRC1 stem-like cells and TNBC MDA-MB-231 cells. Colony formation assays were conducted to evaluate the capacity of individual cells to survive, proliferate and form colonies over an extended period in response to GA treatment. In IDC-derived KAIMRC1 stem-like cells, GA treatment markedly enhanced colony formation in a dose-dependent manner (Fig. 5A-D). Specifically, treatment with 50 μg/ml GA increased colony numbers by 6.77-fold (P=0.0003), whereas 100 μg/ml GA resulted in a 9.01-fold enhancement (P=0.0004) compared

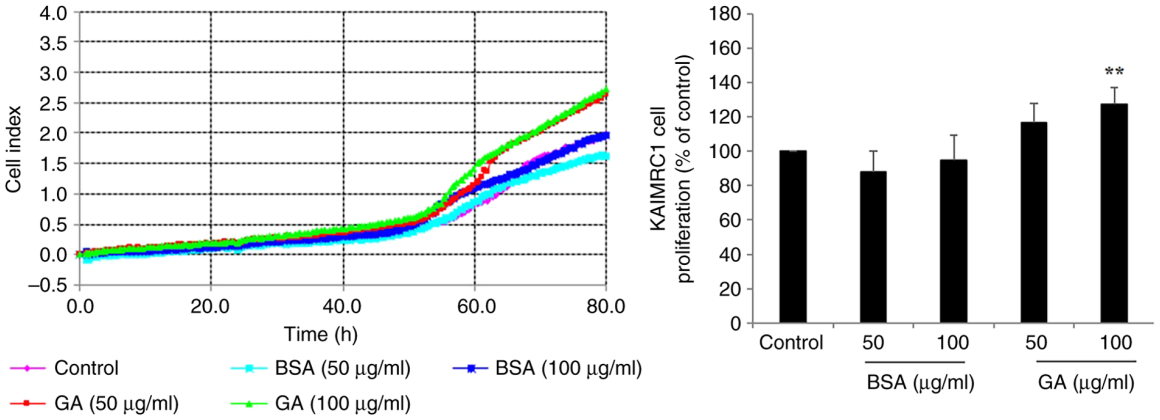

Figure 2. GA effects on the proliferation of invasive ductal carcinoma-derived KAIMRC1 stem-like cells were monitored using an automated xCELLigence Real-Time Cell Analyzer Dual Plate system. Cells were treated with 50-100 μg/ml GA or unglycated BSA for 80 h. Data are presented as the mean ± SD from three independent experiments. Statistical significance relative to the untreated control is indicated as **P<0.01. GA, glycated albumin; BSA, bovine serum albumin.

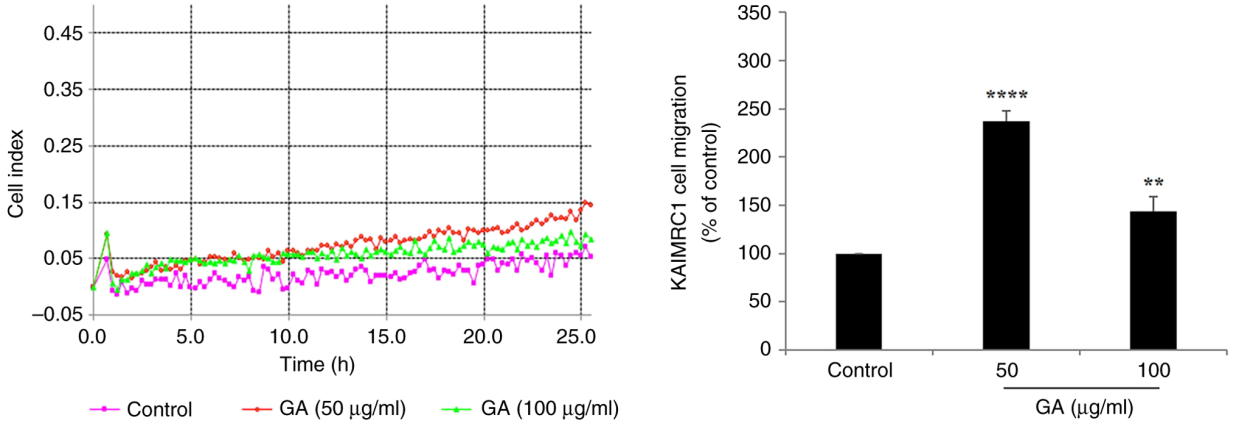

Figure 3. Effects of GA on directional motility of IDC-derived KAIMRC1 stem-like cells were assessed using the Real-time Cell Analyzer Dual Purpose system. The directional motility of KAIMRC1 stem-like cells was quantified following treatment with 50-100 μg/ml GA and compared with that of untreated controls. Data are presented as the mean ± SD from three independent experiments. Statistical significance relative to the untreated control is indicated as **P<0.01 and ****P<0.0001. GA, glycated albumin.

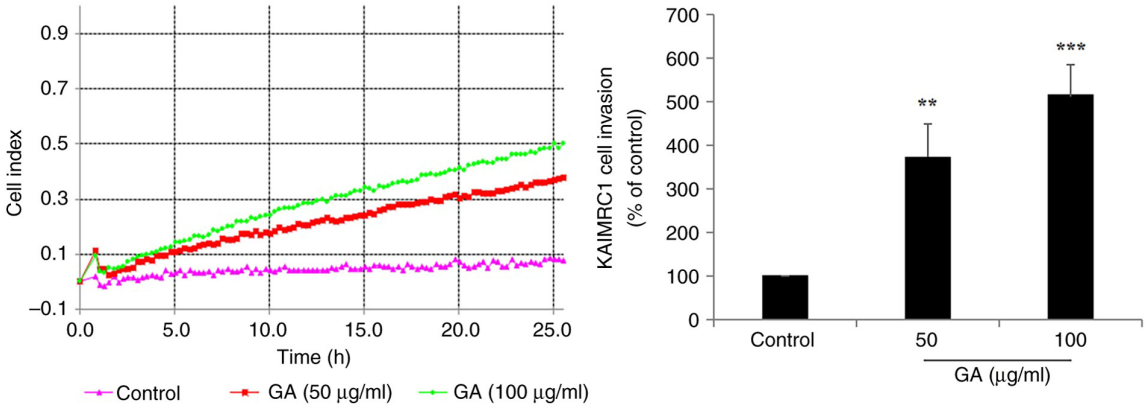

Figure 4. Effects of GA on the invasiveness of invasive ductal carcinoma-derived KAIMRC1 stem-like cells were measured using the automated Real-time Cell Analyzer Dual Purpose system. The invasive capacity of KAIMRC1 stem-like cells was assessed over 24 h following treatment with 50-100 μg/ml of GA and compared with untreated controls. Data are presented as the mean ± SD from three independent experiments. Statistical significance relative to the untreated control is indicated as **P<0.01 and ***P<0.001. GA, glycated albumin.

with untreated controls (Fig. 5D). In TNBC MDA-MB-231 cells, GA also significantly promoted colony formation, although to a lesser extent (Fig. S5). Colony numbers increased by 1.46-fold (P=0.0097) and 1.47-fold (P=0.00099) at 50 and

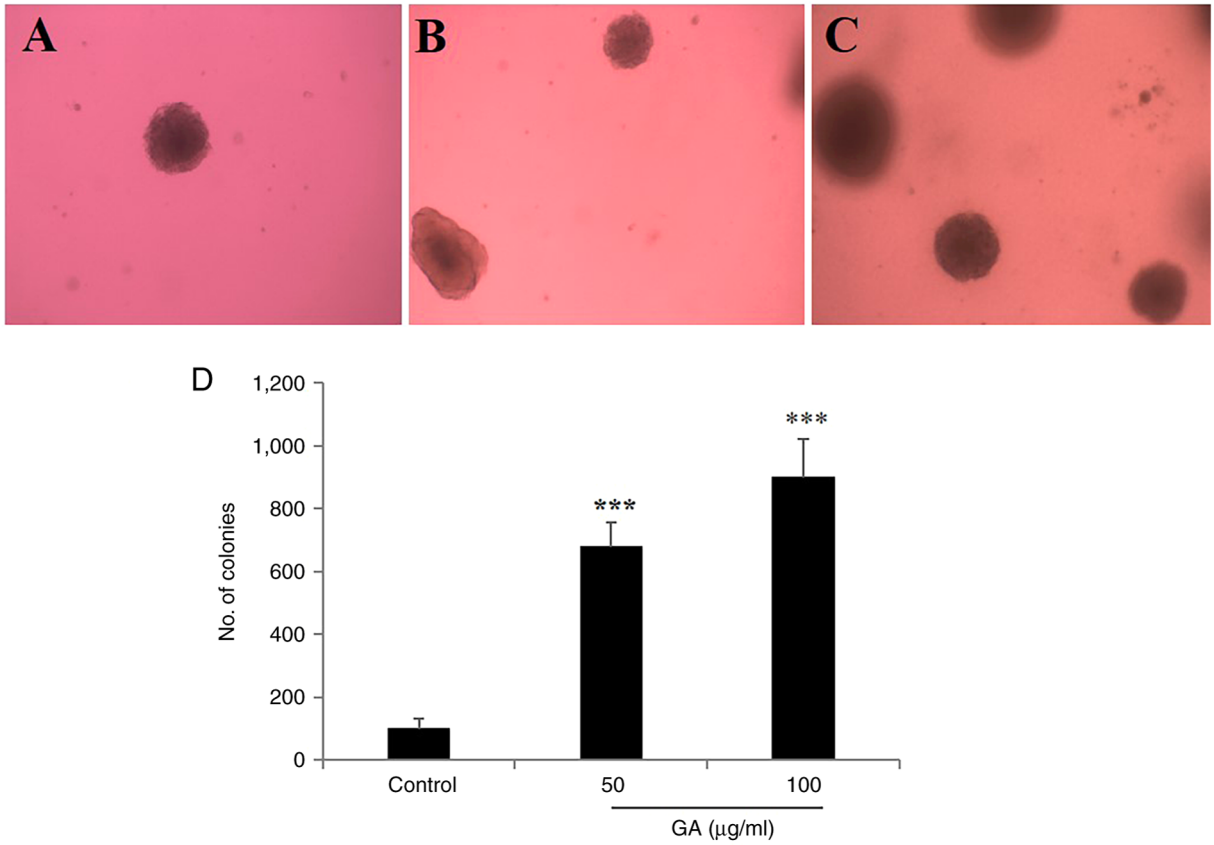

Figure 5. Colony formation of invasive ductal carcinoma-derived KAIMRC1 stem-like cells in the presence of GA. Representative photomicrographs showing the colony formation of KAIMRC1 stem-like cells incubated in the (A) absence or presence of GA tested at (B) 50 μg/ml and (C) 100 μg/ml in soft agar, after 2 weeks. Individual colonies were fixed and counted under microscope (40X objective). (D) Data are presented as the mean ± SD from three independent experiments. Statistical significance relative to the untreated control is indicated as ***P<0.001. GA, glycated albumin.

100 μg/ml, respectively, compared with untreated controls (Fig. S5).

GA induces delayed ERK1/2 phosphorylation in IDC-derived KAIMRC1 stem-like cells. Previous studies using TNBC MDA-MB-231 cells reported that GA induced optimal phosphorylation of the key oncogenic signaling protein ERK1/2 after 10 min exposure to 100 μg/ml GA (38,40), a finding that was corroborated under the present experimental conditions (Fig. S6). In KAIMRC1 stem-like cells, the optimal duration of ERK1/2 phosphorylation was first determined using the same effective GA concentration (100 μg/ml) across multiple incubation periods (30, 60, 90 and 120 min). Upon GA treatment, ERK1/2 phosphorylation level significantly increased at 60 min (5.70-fold for p-ERK1; P=0.0043 and 5.16-fold for p-ERK2; P=0.019) and 90 min (6.50-fold for p-ERK1; P=0.0037 and 6.62-fold for p-ERK2; P=0.0059) compared with untreated control cells, whereas no significant change was observed at 30 and 120 min (Fig. 6A). Based on these results, 90 min was selected as the optimal incubation period for maximal ERK1/2 activation in KAIMRC1 stem-like cells. Subsequently, cells were exposed to increasing concentrations of GA and unglycated BSA (50 and 100 μg/ml) for 90 min. GA induced a significant, concentration-dependent increase in ERK1/2 phosphorylation levels, with a 1.79-fold (P=0.04) increase for p-ERK1 and a 1.78-fold (P=0.047) increase for p-ERK2 at 50 μg/ml, and a 2.81-fold (P=0.016) increase for p-ERK1 and a 1.97-fold (P=0.037) increase for p-ERK2 at 100 μg/ml, compared with untreated control cells (Fig. 6B). Conversely, both concentrations (50 and 100 μg/ml) of unglycated BSA did not alter ERK1/2 phosphorylation levels compared with untreated controls (Fig. 6B).

GA upregulates RAGE, vimentin and OCT3/4 expression in IDC-derived KAIMRC1 stem-like cells and TNBC MDA-MB-231 cells. To determine whether GA stimulates RAGE signaling, induces epithelial-mesenchymal transition (EMT) and promotes stemness features in BC cells, protein expression levels of RAGE, vimentin and OCT3/4 were examined using western blot analysis. Treatment with 100 μg/ml GA markedly increased the expression of all three proteins in both IDC-derived KAIMRC1 stem-like and TNBC MDA-MB-231 cell lines, compared with their basal levels in untreated control cells. In KAIMRC1 stem-like cells, GA treatment significantly elevated the expression of OCT3/4 (1.52-fold; P=0.02), vimentin (1.79-fold; P=0.005) and RAGE (1.68-fold; P=0.012) compared with the basal protein expression levels in untreated control cells (Fig. 7). Similarly, in MDA-MB-231 cells, GA treatment significantly increased the expression of OCT3/4 (1.67-fold; P=0.026), vimentin (2.07-fold; P=0.022) and RAGE (1.56-fold; P=0.044), compared with control cells (Fig. S7). Treatment with unglycated BSA did not alter the expression levels of any of the proteins of interest in either cell line (Figs. 7 and S7).

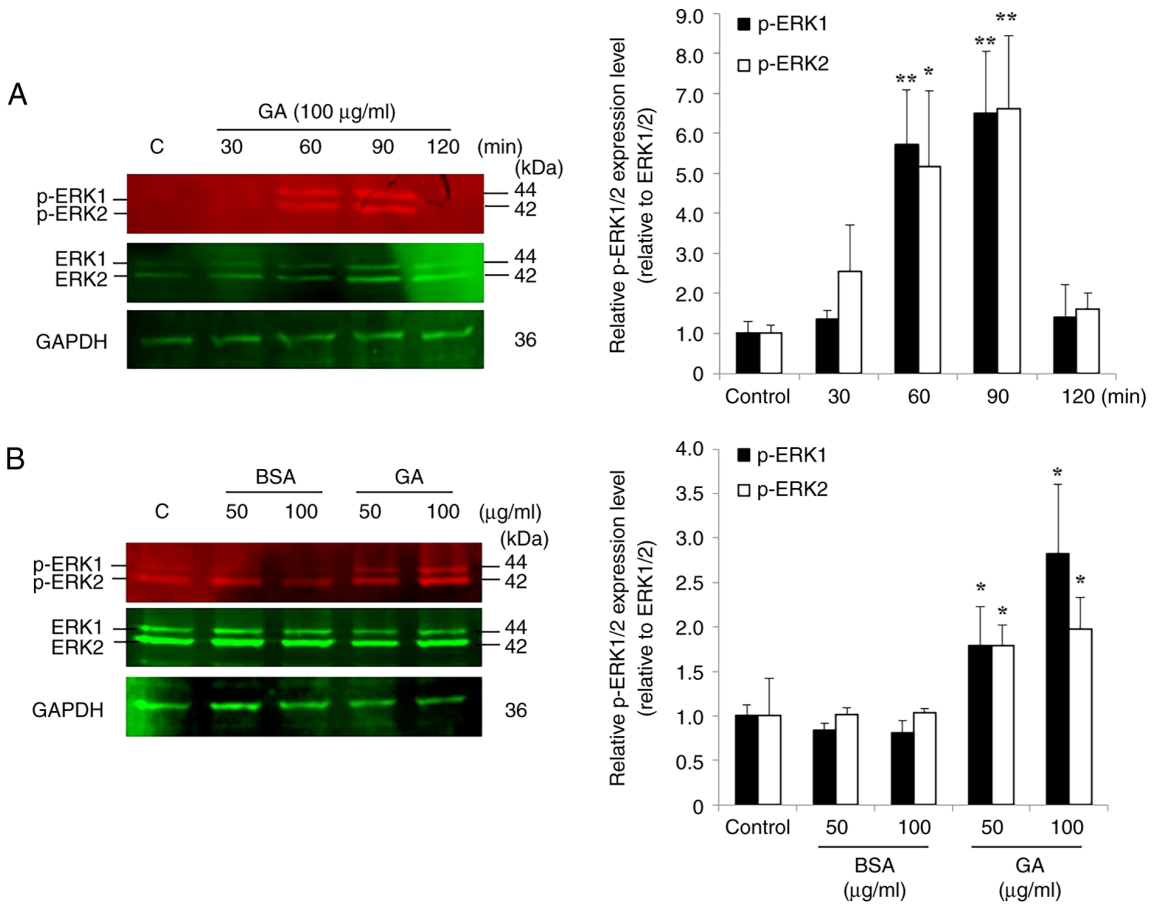

Figure 6. GA effects on ERK1/2 phosphorylation in invasive ductal carcinoma-derived KAIMRC1 stem-like cells. Representative western blot analyses showed p-ERK1/2 in KAIMRC1 stem-like cells treated with 100 μg/ml GA for (A) 30 to 120 min and with (B) 50-100 μg/ml GA or unglycated BSA for 90 min of incubation. Bar graphs show the relative expression level of p-ERK1/2 normalized to total ERK1/2. GAPDH served as the loading control. Data are presented as the mean ± SD from three independent experiments. Statistical significance relative to the untreated control is indicated as *P<0.05 and **P<0.01. C, control; GA, glycated albumin; p-ERK1/2, phosphorylated-ERK1/2; GAPDH, glyceraldehyde 3-phosphate dehydrogenase.

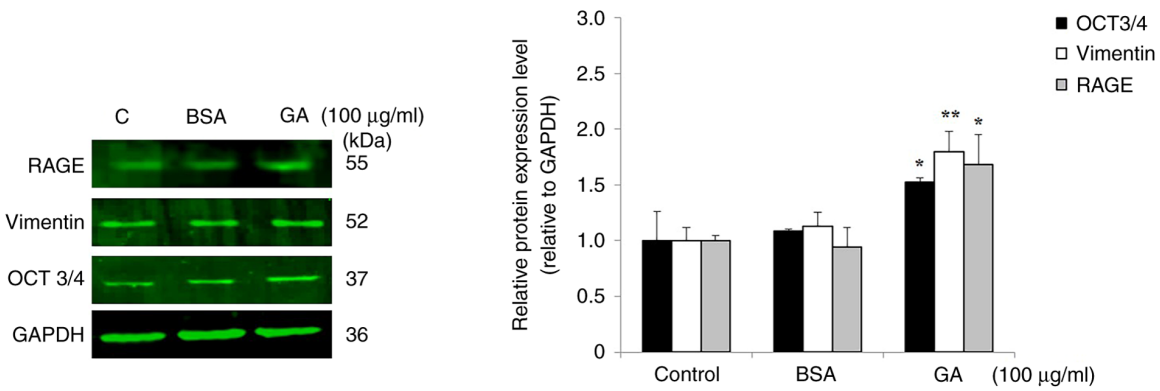

Figure 7. Effects of GA on the expression of RAGE, vimentin and OCT3/4 in invasive ductal carcinoma-derived KAIMRC1 stem-like cells. Representative western blot analyses showing the protein expression levels of RAGE, vimentin and OCT3/4 in KAIMRC1 stem-like cells following 48 h of treatment with 100 μg/ml GA or unglycated BSA, compared with untreated control cells. GAPDH served as the loading control. Bar graphs present the relative protein expression levels normalized to GAPDH. Data are presented as the mean ± SD from three independent experiments. Statistical significance relative to the untreated control group is indicated as *P<0.05 and **P<0.01. RAGE, receptor for advanced glycation end products; GA, glycated albumin; BSA, bovine serum albumin; GAPDH, glyceraldehyde 3-phosphate dehydrogenase.

Bioinformatics analysis reveals elevated VIM gene expression in invasive breast carcinoma, TNBC and ER^{+}/HER2^{-} tumors, associated with reduced 5-year survival. Gene expression levels of RAGE (*AGER*), vimentin (*VIM*) and OCT4 (*POU5F1*) were evaluated utilizing data from the SCAN-B dataset within the MammOnc-DB database (43,44). Analysis by biopsy type (Fig. 8A) showed that *AGER* and *VIM* were significantly higher in invasive carcinoma (n=7,880) compared

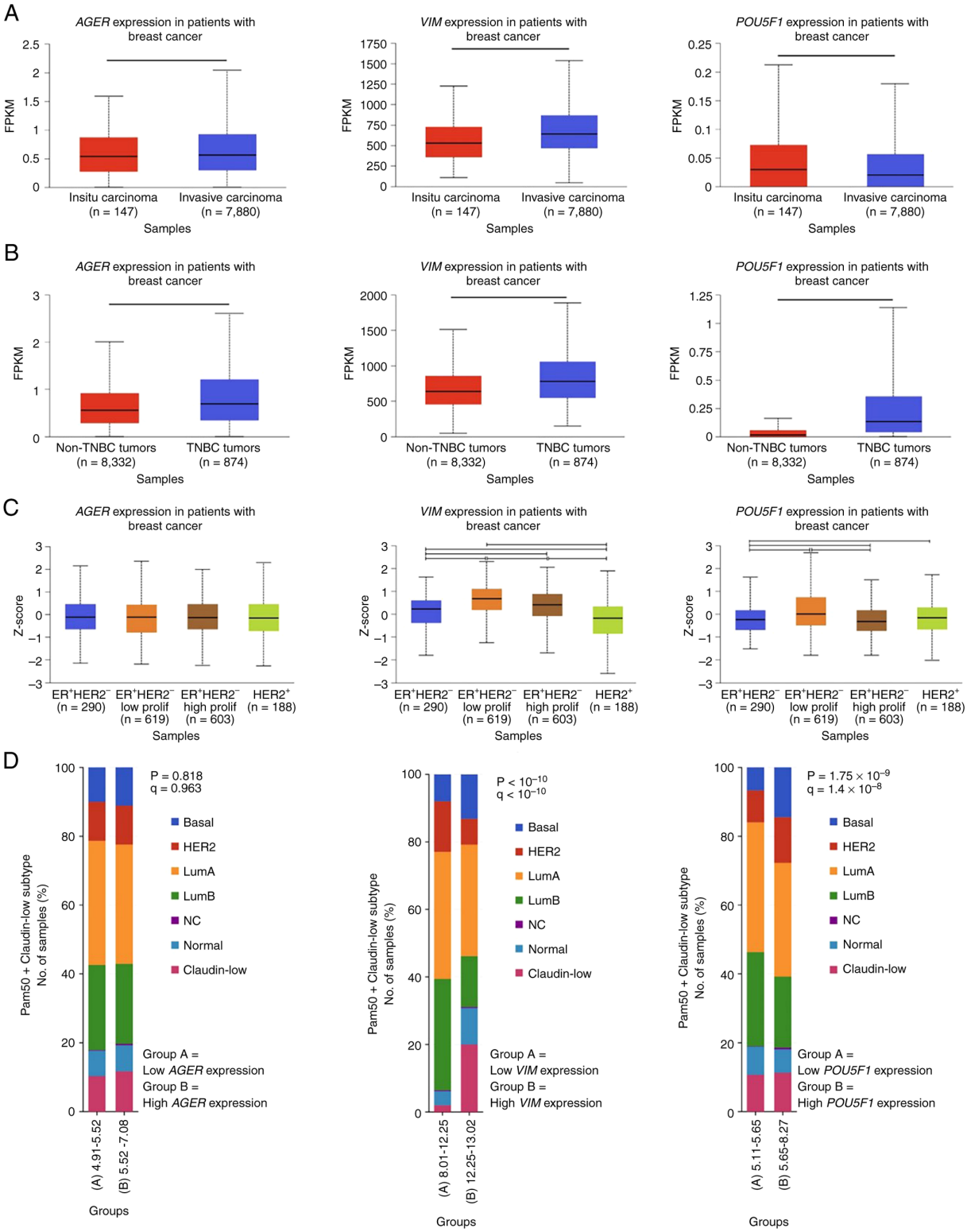

Figure 8. Bioinformatics analysis of databases from patients with BC. (A) Increased mRNA expression levels of RAGE (*AGER*) and vimentin (*VIM*) in patients with BC and invasive carcinoma. (B) Upregulated mRNA expression of *AGER*, *VIM* and OCT4 (*POU5F1*) in TNBC patients. (C) Elevated mRNA levels of *VIM* and *POU5F1* in patients with ER^+HER2^- low-proliferative tumors. (D) Molecular profiling using PAM50 classified BC intrinsic subtypes based on the expression patterns of 50 genes and 8 housekeeping genes. Higher *VIM* mRNA expression with increased percentage of basal and claudin-low subtypes, whereas increased *POU5F1* mRNA levels were associated with a higher percentage of the basal subtype. FPKM fragments per kilobase of transcripts per million mapped reads; TNBC, triple-negative breast cancer; low prolif, low proliferative; high prolif, high proliferative; PAM50, prediction analysis of microarray 50.

with carcinoma *in situ* (n=147; $P=2.2x10^{-2}$ and $P=3.35x10^{-3}$; respectively). Further analysis (Fig. 8B) indicated that patients with TNBC (n=874) exhibited significantly higher mRNA levels of *AGER*, *VIM* and *POU5F1* than those without TNBC (n=8,332; $P<1x10^{-12}$). Gene expression profiles stratified by three-gene classifier subtypes from the METABRIC dataset

were also examined (43,45). Patients with BC were categorized as ER^-HER2^- (n=290), ER^+HER2^- low proliferative (n=619), ER^+HER2^- high proliferative (n=603) and $HER2^+$ (n=188). Fig. 8C indicates that patients with ER^+HER2^- low-proliferative tumors had significantly higher *VIM* and *POU5F1* mRNA levels than patients with ER^-HER2^- subtype ($P=4.99x10^{-7}$ and $P=1.63x10^{-10}$, respectively). Comparative analysis of gene expression based on PAM50 and claudin subtypes using the 'Breast Cancer (METABRIC, Nature 2012 & Nat Commun 2016)' dataset from cBioPortal (45-50) revealed that P with high *VIM* expression were enriched in basal and claudin-low subtypes ($P<1x10^{-10}$), whereas elevated *POU5F1* expression was primarily associated with the basal subtype ($P=1.75x10^{-9}$; Fig. 8D). Survival analysis using SCAN-B dataset indicated that patients with BC with low-to-moderate *VIM* (n=1,935) or *POU5F1* (n=1,935) expression had significantly favourable 5-year survival (P=0.018 and P<0.0001, respectively), whereas *AGER* expression did not notably affect the survival of patients with BC (Fig. 9).

Bioinformatics analysis indicates elevated mRNA expression levels of VIM, AGER and POU5F1 in patients with BC and T2DM. Panigrahi *et al* (51) examined 73 patients with BC, including 36 patients with DM and 37 without DM. The diabetic group was further stratified into T1DM (n=6) and T2DM (n=30). *VIM* mRNA expression was significantly higher in patients with DM when compared with those without DM, with the most pronounced increase in patients with T2DM (Mann-Whitney U test; P=0.003; Fig. 10A). Although pairwise comparisons did not reach statistical significance, a small increase in *POU5F1* (Fig. 10B) and *AGER* (Fig. 10C) mRNA expressions were observed in the diabetic group, particularly in the T2DM counterparts. A correlation heatmap (Fig. S8) illustrating expression profiles of *VIM*, *POU5F1* and *AGER* across all patients showed marked differences in *VIM* expression between patients with BC with and without DM. Conversely, no discernible differences were observed for *POU5F1* and *AGER* expression (Fig. S8).

GA upregulates vimentin protein expression in IDC-derived KAIMRC1 stem-like and TNBC MDA-MB-231 cells through RAGE. To determine whether GA activates KAIMRC1 stem-like and MDA-MB-231 cells through the RAGE signaling pathway, cells were pretreated with a neutralizing anti-RAGE antibody to inhibit RAGE signaling or with an IgG isotype control antibody as a negative control. Cells were exposed to 100 μg/ml GA for 48 h of incubation. This approach allowed assessment of whether RAGE is required for the cellular response to GA stimulation. As shown in Fig. 11, treatment with GA significantly increased vimentin expression in KAIMRC1 stem-like cells (1.64-fold; P=0.045; Fig. 11) and MDA-MB-231 cells (1.39-fold; P=0.012; Fig. S9) pretreated with the IgG control antibody, compared with untreated controls. Conversely, GA-induced vimentin upregulation was not observed in either cell line when RAGE signaling was blocked by pretreatment with an anti-RAGE antibody (Figs. 11 and S9).

Discussion

Management of patients with T2DM who develop IDC remains suboptimal, partly because these patients often present at advanced stages and frequently develop aggressive TNBC (11,53,54). Challenges include late detection and the limited effectiveness of currently available systemic treatments, including chemotherapy and immunotherapy (55). CSCs, identified in both TNBC and IDC tissues, have garnered considerable interest in clinical research because they represent a small population of undifferentiated tumor cells associated with tumor onset, metastasis, therapy resistance and recurrence (28). KAIMRC1, a spontaneously immortalized BC cell line derived from the surgical biopsy of a Saudi female patient diagnosed with IDC was previously established and characterized (33). Notably, these cells exhibit CSC-associated phenotypes and CSC markers, including $CD24^-/CD44^+$, CD47 and ALDH1 (33). However, molecular evidence associating GA, the most abundant globular circulating glycated protein used as a clinical biomarker for DM (56), to the best of our knowledge, CSC-associated tumorigenesis in BC remains limited. MG was used for the generation of GA however, due to its low expression in TNBC compared with other BC subtypes (57), the biological effects of MG were not investigated in the present study. Thus, the pro-tumorigenic effects of GA on IDC-derived KAIMRC1 stem-like cells compared with MDA-MB-231 cells, a mature and heterogeneous TNBC cell line known to contain a CSC subpopulation were explored (58). A detailed examination of the functional and molecular characteristics of BCSCs under hyperglycemic conditions may help identify new biomarkers and molecular targets, ultimately supporting the early detection and targeted therapeutic strategies for patients with T2DM and invasive BC.

Stemness properties in IDC-derived KAIMRC1 cells were initially assessed by comparing ALDH activity with that of the poorly differentiated TNBC cell line MDA-MB-231. ALDH is a highly active enzyme in both normal stem cells and CSCs, where it contributes to key stem cell properties, including self-renewal, differentiation and drug resistance, and is considered a potential therapeutic and prognostic marker (52,59,60). In the present study, IDC-derived KAIMRC1 cells exhibited significantly higher ALDH activity when compared with MDA-MB-231 cells. However, a previous study reported higher cell surface expression of the CSC-associated protein ALDH1 on MDA-MB-231 cells when compared with that on KAIMRC1 cells (33). KAIMRC1 cells were previously shown to possess CSC-like properties, including robust spheroid formation in soft agar (33). In the present study, the elevated ALDH activity observed in KAIMRC1 cells further emphasizes their relevance as a model for studying BC stemness under hyperglycemic conditions, compared with MDA-MB-231 cells, a TNBC model frequently associated with T2DM-related BC (16).

At the functional and tumorigenic levels, GA significantly enhanced cell proliferation, motility, invasion, colony formation and ERK1/2 phosphorylation in both IDC-derived KAIMRC1 stem-like and TNBC MDA-MB-231 cells, although the magnitude and timing of these responses varied between the two models. In MDA-MB-231 cells, GA exhibited a bell-shaped, dose-dependent proliferation response, with an optimal effect at 100 μg/ml, indicating the involvement of a dimeric receptor such as RAGE. These findings are consistent with a previous study reporting that GA at 100 μg/ml enhances TNBC MDA-MB-231 cell proliferation,

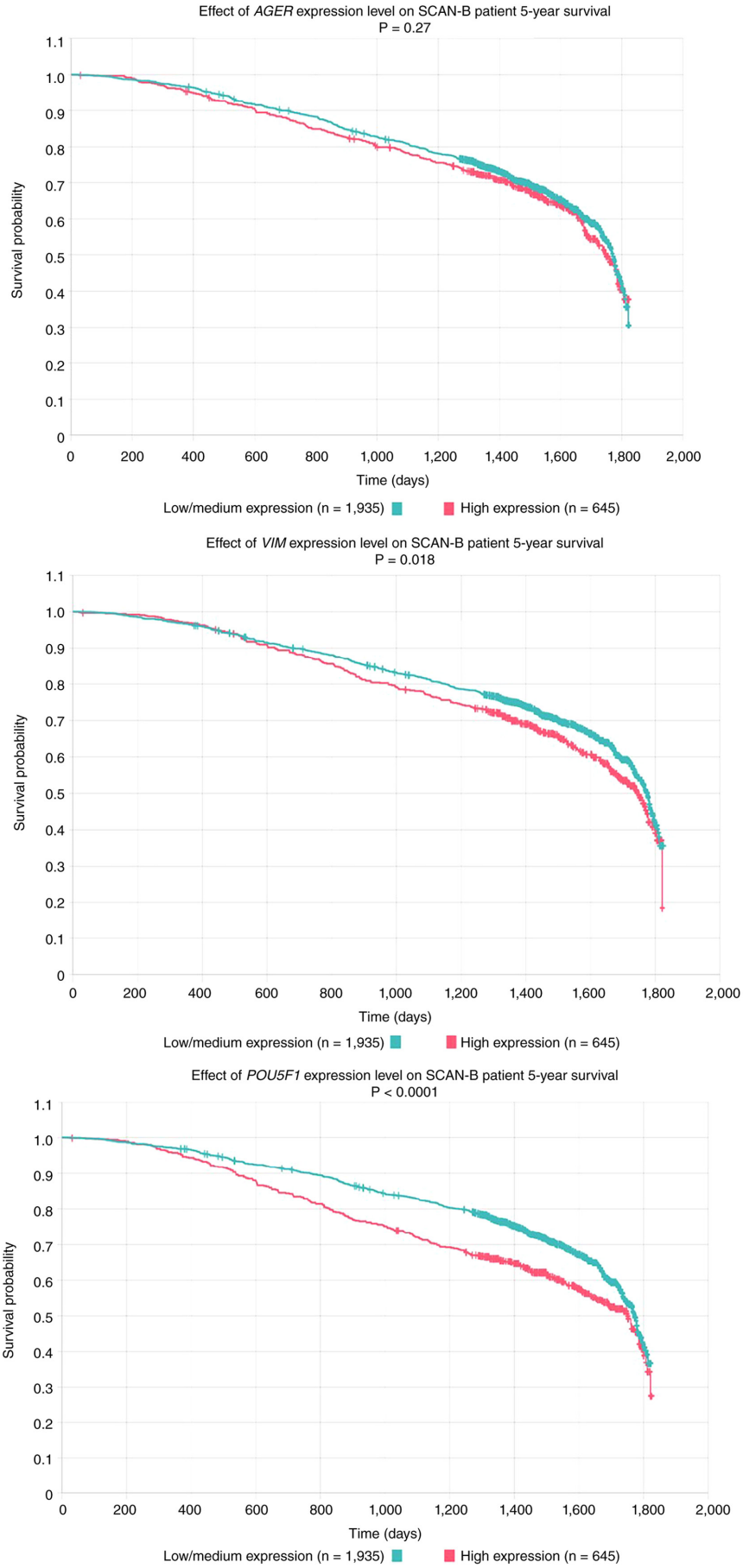

Figure 9. Effects of *AGER* (top), *VIM* (middle) and *POU5F1* (bottom) gene expression levels on 5-year survival in patients from SCAN-B. Lower or intermediate mRNA expression levels of *VIM* and *POU5F1* was associated with improved 5-year survival in patients with breast cancer. The data were obtained from the SCAN-B study within the MammOnc-DB database (43,41). SCAN-B, Swedish Cancerome Analysis Network-Breast.

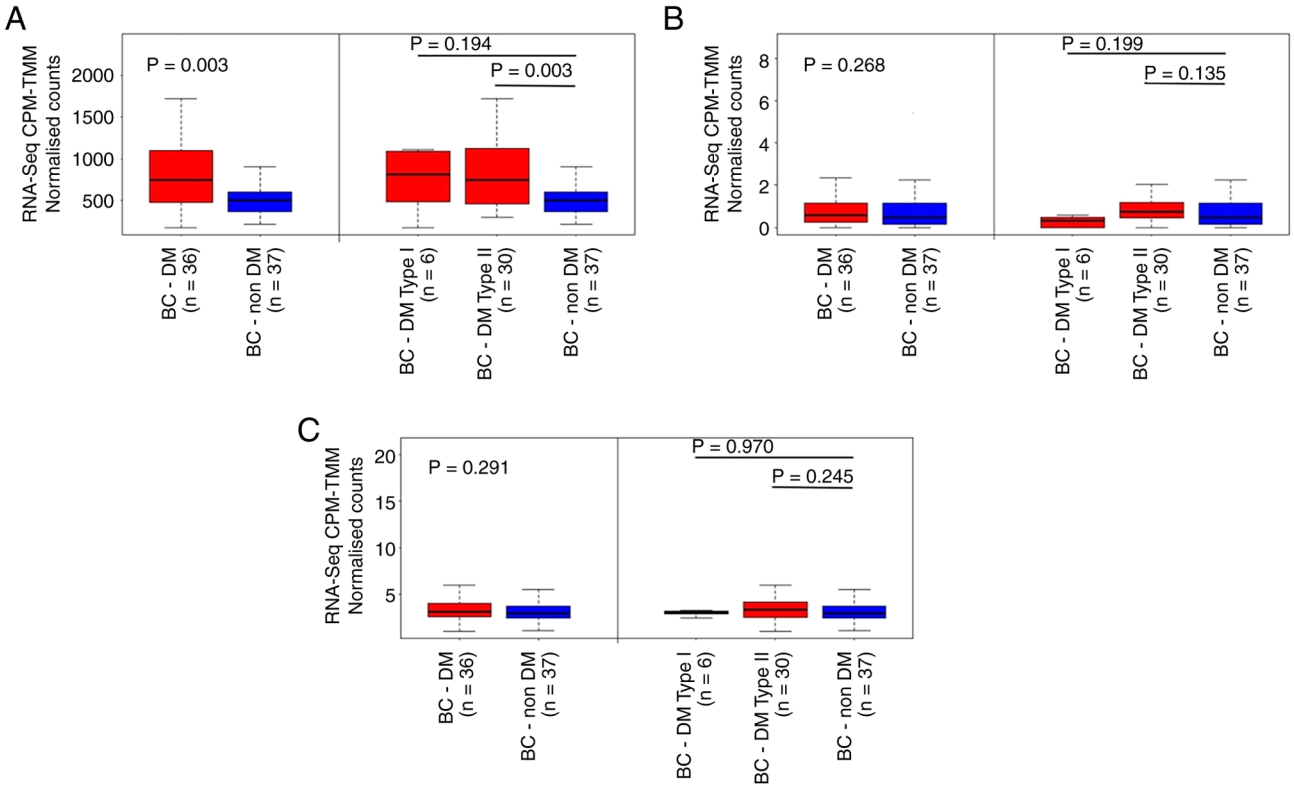

Figure 10. Upregulation of (A) *VIM*, (B) *POU5F1* and (C) *AGER* mRNA levels in patients with BC with DM. Higher expression was particularly observed in those with T2DM compared with those without DM. Pairwise comparisons were conducted using the Mann-Whitney U test. The data were obtained from the study of Panigrahi *et al* (51). BC, breast cancer; DM, diabetes mellitus; T1DM, type 1 diabetes mellitus; T2DM, type 2 diabetes mellitus, RNA-seq, RNA sequencing; CPM-TMM, counts per million after trimmed mean of M-values, FPKM, fragments per kilobase of transcript per million mapped reads.

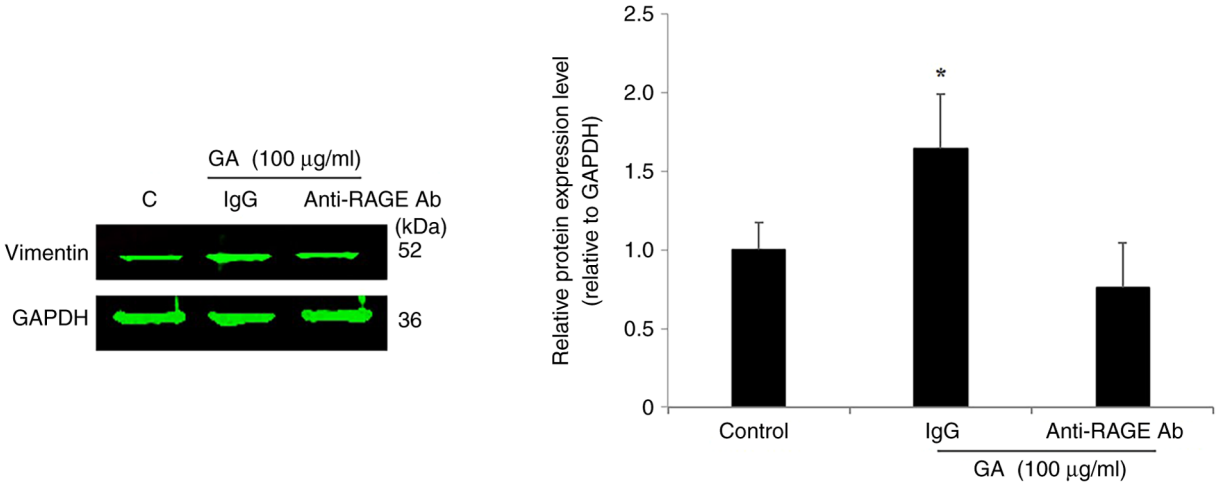

Figure 11. RAGE mediates GA-induced upregulation of vimentin in invasive ductal carcinoma-derived KAIMRC1 stem-like cells. Western blot analyses showed that blocking RAGE with a neutralizing anti-RAGE antibody prevented GA-induced vimentin expression in KAIMRC1 stem-like cells compared with cells pretreated with an IgG1 isotype control. Bar graphs present the semi-quantified vimentin expression levels normalized to GAPDH. Data are presented as the mean ± SD from three independent experiments. Statistical significance relative to the untreated control group is indicated as $^{*}P<0.05$. GA, glycated albumin; RAGE, receptor for advanced glycation end products; GAPDH, glyceraldehyde 3-phosphate dehydrogenase.

migration and invasion, accompanied by increased MMP-9 gelatinase activity mediated through RAGE, using other *in vitro* cell-based assays such as trypan blue exclusion, scratch wound and Boyden chamber assays (38). In the present study, GA also significantly increased the proliferation of IDC-derived KAIMRC1 stem-like cells, although to a lesser extent than that in TNBC MDA-MB-231 cells, indicating a comparatively slower proliferative rate. This observation is consistent with the well-recognized tendency of adult CSCs to remain in a quiescent phase to preserve long-term self-renewal potential and minimize replication-associated errors (61).

The biological effects of GA on cell motility and, notably, on the ability to cross a reconstituted basement membrane revealed that IDC-derived KAIMRC1 stem-like cells were

more responsive than TNBC MDA-MB-231 cells. Although TNBC cells are highly invasive, CSCs are well known for their metastatic potential, and previous mechanobiology studies have shown that they exhibit markedly elevated invasive potential (62,63). These findings suggest that GA may play an important role in increasing CSC invasiveness, a hallmark of metastatic progression and an indicator of tumor aggressiveness. Additionally, a BC invasion scoring model was recently developed to predict tumor aggressiveness, therapeutic response and prognosis by analyzing the PAM pathway (64). Phosphorylation of p70S6K1, the downstream effector of the PAM pathway, was detected in IDC tissues from patients with T2DM, and pharmacological inhibition of p70S6K1 using PF-4708671 suppressed GA-induced invasion in TNBC (14,40). These findings indicate that additional modeling of PAM/p70S6K1 pathway in patients with T2DM diagnosed with IDC or TNBC may help refine predictions of clinical outcomes, including recurrence and therapeutic responses.

From a tumorigenic standpoint, the present findings reveal that GA significantly enhanced colony-forming ability in both KAIMRC1 stem-like cells and MDA-MB-231 cells. The clonogenic assay is a quantitative *in vitro* method used to evaluate the capacity of a single cell to undergo clonal expansion and form a colony, thereby reflecting tumorigenic potential (65,66). In the present study, treatment with GA produced more colonies in KAIMRC1 stem-like cells when compared with that in the more differentiated MDA-MB-231 cells, indicating a potent tumorigenic effect in CSCs-enriched cells. Consistent with these findings, a commercial AGE-BSA at 40-80 μg/ml promoted colony formation in human primary TNBC cells (67). Additionally, several AGEs-BSA preparations, including MG-derived AGEs, have been shown to exert pro-tumorigenic effects in prostate cancer cells and xenografts mouse models, accompanied by RAGE overexpression and increased levels of EMT markers, including N-cadherin and vimentin (68). Verification of the tumorigenic potential of GA on IDC-derived KAIMRC1 stem-like cells could be strengthened using *in vivo* models, such as xenografts mouse models.

Focusing on the main signaling oncoprotein ERK1/2, GA was shown to transiently activate the ERK1/2 signaling pathway in TNBC MDA-MB-231 cells and IDC-derived KAIMRC1 stem-like cells. Previous studies reported that, in MDA-MB-231 cells, ERK1/2 phosphorylation peaks rapidly, ~10 min posttreatment with an effective concentration of GA, and exhibits a characteristic bell-shaped response, indicating the involvement of the dimeric receptor RAGE (38,40). Additional *in vitro* studies have confirmed that ERK signaling is a key component of the AGEs-RAGE axis promoting carcinogenesis (67,69,70). In contrast to the rapid response observed in MDA-MB-231 cells, KAIMRC1 stem-like cells exhibited delayed ERK1/2 activation, with phosphorylation significantly increasing only after 60-90 min of treatment with GA. Notably, stem-like cells, including those exhibiting mesenchymal features, often show altered sensitivity to external stimuli due to their unique epigenetic and signaling profiles (71,72). Therefore, the delayed phosphorylation response in KAIMRC1 stem-like cells may reflect differences from mature cancer cells in membrane receptor expression, intracellular signaling dynamics or metabolic activity.

The regulatory role of GA in key stemness markers, such as OCT3/4 and vimentin, was also examined. The present results revealed that treatment with GA induced a significant upregulation of mesenchymal markers OCT3/4 and vimentin in both IDC-derived KAIMRC1 stem-like cells and TNBC MDA-MB-231 cells compared with untreated controls. These findings are consistent with clinical reports indicating that T2DM promotes differentiation of mesenchymal stem cells (MSCs), particularly adipose tissue-derived MSCs, generating MSC-derived extracellular vesicles in the blood circulation, that contribute to BC metastasis (73,74). *In vivo* experimental evidence from diabetic mouse models has similarly shown that hyperglycemia induces a mesenchymal phenotype in BC cells, thereby increasing their motility and invasive potential (75). OCT3/4 is a transcription factor that plays a key role in expressing and maintaining pluripotency and self-renewal (76). Reactivation of OCT3/4 expression has been observed in several human BC cell lines but not in non-malignant cells (77). Notably, previous studies have shown that OCT4 expression in CSC promotes colony formation, metastasis and cancer progression, as shown in human cervical and liver cancer models (78,79). Consistent with these findings, the present data suggest that GA-induced elevation of OCT3/4 may mediate greater enhancement of colony formation in KAIMRC1 stem-like cells when compared with that in MDA-MB-231 cells. Vimentin, a pivotal cytoskeletal protein typically associated with mesenchymal cells, is a key marker of EMT (80). EMT mechanisms are essential for improving cancer cell invasion and migration, which are key factors influencing metastatic potential (81). In the present study, GA-induced vimentin overexpression coincided with augmented invasiveness and motility in both cell lines. Furthermore, elevated vimentin expression was observed in patients with TNBC and in $ER^+/HER2^-$ subtypes, including the cellular model KAIMRC1, associating with poor-prognosis in patients with T2DM diagnosed with BC compared with those without DM. These findings corroborate previous clinical studies reporting that vimentin is a poor prognostic biomarker and therapeutic target in patients with BC and TNBC, primarily due to its involvement in tumor progression and metastasis (82,83).

Furthermore, using the invasive BC cell line SK-BR3, metformin was shown to suppress vimentin expression (84). It would therefore be beneficial to monitor vimentin expression in patients with T2DM diagnosed with invasive BC and determine overall survival. Importantly, RAGE neutralization significantly inhibited GA-induced enhancement of vimentin expression, indicating that RAGE is an important mediator of GA-driven EMT and potentially stemness-related phenotypes. This observation aligns with prior evidence suggesting that AGEs, particularly GA, modulate EMT processes through RAGE-dependent mechanisms (26). Other research tools such as small interfering RNA technology could be applied to verify and strengthen the key role of RAGE signaling in GA-induced vimentin expression. Additionally, an *in silico* analysis of the publicly available gene expression data from Panigrahi *et al* (51) was conducted on 36 patients with DM and 37 without DM. The small sample size may constrain the ability to draw statistically significant or clinically meaningful conclusions, particularly when considering potential confounding factors such as disease duration, severity, HbA1c levels and treatment regimens. To the best of our knowledge, no other publicly available diabetic BC

datasets of sufficient sample size exist to allow further *in silico* validation. Despite this limitation, the analyzed dataset offers valuable preliminary insights that warrant further exploration. These findings underscore the importance of monitoring the gene expression levels of *VIM, POU5F1 and AGER* in local Saudi cohorts of patients with BC and with DM.

In conclusion, the present study showed that GA stimulates key tumorigenic and stemness-associated properties in IDC-derived KAIMRC stem-like cells and TNBC MDA-MB-231 cells, representing *in vitro* models of BC subtypes prevalent in patients with T2DM. GA primarily promotes proliferation in the poorly differentiated MDA-MB-231 cell line, while concurrently enhancing stemness-associated features, motility, invasiveness and EMT in the KAIMRC1 stem-like cell line. These effects are mediated through the RAGE signaling pathway, as evidenced by the reduction in GA-induced vimentin upregulation following RAGE neutralization. Bioinformatics analyses further indicate that low vimentin expression is associated with improved overall survival in patients with T2DM and BC. Although additional *in vitro* studies in primary IDC-derived BC cells are warranted, these findings highlight the AGEs-RAGE axis as a key mechanism linking hyperglycemia to enhanced stemness in IDC-derived BCSCs and TNBC. Notably, vimentin emerges as a potential prognostic biomarker, and targeting the AGEs-RAGE pathway may represent a viable therapeutic strategy. Further clinical research on the impact of *VIM* transcript levels and their associations with overall survival in patients with T2DM with invasive BC is necessary to validate its prognostic utility.

Acknowledgements

Not applicable.

Authors' contributions

SMN conceived and conducted the study. SMN and RaA supervised the study, analysed and interpreted the data, and reviewed the manuscript. MA, NA, SH, ReA and RiA performed the experiments, generated the data, collected the data and reviewed the manuscript. MKA and AA carried out bioinformatics analyses. MA, MKA, AAA and SMN interpreted the data, wrote and reviewed the manuscript. SMN and MKA confirm the authenticity of all the raw data. All authors read and approved the final manuscript.

Funding

This work was supported by King Abdullah International Medical Research Center (grant no. SP24R/018/01).

Availability of data and materials

The data generated in the present study may be requested from the corresponding author.

Ethics approval and consent to participate

Not applicable.

Patient consent for publication

Not applicable.

Competing interests

The authors declare that they have no competing interests.

References

1. Lu X, Xie Q, Pan X, Zhang R, Zhang X, Peng G, Zhang Y, Shen S and Tong N: Type 2 diabetes mellitus in adults: Pathogenesis, prevention and therapy. Signal Transduct Target Ther 9: 262, 2024.
2. IDF Diabetes Atlas 2025 (IDF). IDF, Brussels, 2025. https://diabetesatlas.org/resources/idf-diabetes-atlas-2025/
3. GBD 2021 Diabetes Collaborators: Global, regional, and national burden of diabetes from 1990 to 2021, with projections of prevalence to 2050: A systematic analysis for the global burden of disease study 2021. Lancet 402: 203-234, 2023.
4. Robertson CC, Elgamal RM, Henry-Kanarek BA, Arvan P, Chen S, Dhawan S, Eizirik DL, Kaddis JS, Vahedi G, Parker SCJ, *et al*: Untangling the genetics of beta cell dysfunction and death in type 1 diabetes. Mol Metab 86: 101973, 2024.
5. Młynarska E, Czarnik W, Dzieża N, Jędraszak W, Majchrowicz G, Prusinowski F, Stabrawa M, Rysz J and Franczyk B: Type 2 diabetes mellitus: New pathogenetic mechanisms, treatment and the most important complications. Int J Mol Sci 26: 1094, 2025.
6. Petrović N, Milosavljević M, Gojak R, Đešević M, Lakić D, Stević I and Janković S: Costs of treating type 2 diabetes mellitus and its complications. Biotechnol Biotchnol Equip 38: 2399941, 2024.
7. Zhang YY, Li YJ, Xue CD, Li S, Gao ZN and Qin KR: Effects of T2DM on cancer progression: Pivotal precipitating factors and underlying mechanisms. Front Endocrinol (Lausanne) 15: 1396022, 2024.
8. Alshammari AM, Elnaem MH and Ong SC: Evaluating the economic impact of diabetes mellitus: A hospital-centric cost analysis in Hail, Saudi Arabia. Clinicoecon Outcomes Res 17: 473-484, 2025.
9. Wen S, Yuan Y, Li Y, Xu C, Chen L, Ren Y, Wang C, He Y, Li X, Gong M, *et al*: The effects of non-insulin anti-diabetic medications on the diabetic microvascular complications: a systematic review and meta-analysis of randomized clinical trials. BMC Endocr Disord 25: 179, 2025.
10. Hao Q, Huang Z, Li Q, Liu D, Wang P, Wang K, Li J, Cao W, Deng W, Wu K, *et al*: A novel metabolic reprogramming strategy for the treatment of diabetes-associated breast cancer. Adv Sci (Weinh) 9: e2102303, 2022.
11. Lu Y, Hajjar A, Cryns VL, Trentham-Dietz A, Gangnon RE, Heckman-Stoddard BM and Alagoz O: Breast cancer risk for women with diabetes and the impact of metformin: A meta-analysis. Cancer Med 12: 11703-11718, 2023.
12. Kounatidis D, Vallianou NG, Karampela I, Rebelos E, Kouveletsou M, Dalopoulos V, Koufopoulos P, Diakoumopoulou E, Tentolouris N and Dalamaga M: Anti-diabetic therapies and cancer: From bench to bedside. Biomolecules 14: 1479, 2024.
13. Vulichi SR, Runthala A, Begari N, Rupak K, Chunduri VR, Kapur S, Chippada AR and Sistla DSM: Type-2 diabetes mellitus-associated cancer risk: In pursuit of understanding the possible link. Diabetes Metab Syndr 16: 102591, 2022.
14. Matou-Nasri S, Aldawood M, Alanazi F and Khan AL: Updates on triple-negative breast cancer in type 2 diabetes mellitus patients: From risk factors to diagnosis, biomarkers and therapy. Diagnostics (Basel) 13: 2390, 2023.
15. Durrani IA, John P, Bhatti A and Khan JS: Network medicine based approach for identifying the type 2 diabetes, osteoarthritis and triple negative breast cancer interactome: Finding the hub of hub genes. Heliyon 10: e36650, 2024.
16. Liu L, Gao Y, Liu P, Hui R and Zhang J: Association of type 2 diabetes mellitus with histopathological features of non-metastatic breast cancer in Chinese women: A retrospective Cross-sectional study. Sci Rep 15: 28645, 2025.
17. Bray F, Laversanne M, Sung H, Ferlay J, Siegel RL, Soerjomataram I and Jemal A: Global cancer statistics 2022: GLOBOCAN estimates of incidence and mortality worldwide for 36 countries in 185 countries. CA Cancer J Clin 74: 229-263, 2024.

18. Lawrenson R, Lao C, Stanley J, Teng A, Kuper-Hommel M, Campbell I, Krebs J, Sika-Paotonu D, Koea J, Meredith I and Gurney J: Does diabetes affect breast cancer survival? Cancer Rep (Hoboken) 7: e2040, 2024.
19. Natalicchio A, Marrano N, Montagnani M, Gallo M, Faggiano A, Zatelli MC, Argentiero A, Del Re M, D'Oronzo S, Fogli S, *et al*: Glycemic control and cancer outcomes in oncologic patients with diabetes: An Italian Association of Medical Oncology (AIOM), Italian Association of Medical Diabetologists (AMD), Italian Society of Diabetology (SID), Italian Society of Endocrinology (SIE), Italian Society of Pharmacology (SIF) multidisciplinary critical view. J Endocrinol Invest 47: 2915-2928, 2024.
20. Sears AJ, Wild SH, Mesa-Eguiagaray I, Hall PS and Figueroa JD: Breast cancer survival and mortality among women with type 2 diabetes: A retrospective cohort study. Sci Rep 15: 26144, 2025.
21. Jordt N, Kjærgaard KA, Thomsen RW, Borgquist S and Cronin-Fenton D: Breast cancer and incidence of type 2 diabetes mellitus: A systematic review and meta-analysis. Breast Cancer Res Treat 202: 11-22, 2023.
22. Ahmed SBM, Radwan N, Amer S, Sharif-Askari NS, Mahdami A, Samara KA, Halwani R and Jelinek HF: Assessing the link between diabetic metabolic dysregulation and breast cancer progression. Int J Mol Sci 24: 11816, 2023.
23. Zhang AMY, Xia YH, Lin JSH, Chu KH, Wang WCK, Ruiter TJJ, Yang JCC, Chen N, Chhuor J, Patil S, *et al*: Hyperinsulinemia acts via acinar insulin receptors to initiate pancreatic cancer by increasing digestive enzyme production and inflammation. Cell Metab 35: 2119-2135.e5, 2023.
24. Wang W, Hapach LA, Taufalele PV, Bates ME, Wu Y and Reinhart-King C: Diabetic hyperglycemia-induced glycation regulates tumor vasculature integrity via NF-kB-mediated GM-CSF secretion by tumor cells. Cell Biomater 1: 100186, 2025.
25. Vella V, Lappano R, Bonavita E, Maggiolini M, Clarke RB, Belfiore A and De Francesco EM: Insulin/IGF axis and the receptor for advanced glycation end products: Role in meta-inflammation and potential in cancer therapy. Endocr Rev 44: 693-723, 2023.
26. Coser M, Neamtu BM, Pop B, Cipaian CR and Crisan M: RAGE and its ligands in breast cancer progression and metastasis. Oncol Rev 18: 1507942, 2025.
27. Oliveira RV, Souza VB, Souza PC, Soares FA, Vassallo J, Rocha RM and Schenka AA: Detection of putative stem-cell markers in invasive ductal carcinoma of the breast by immunohistochemistry: Does it improve prognostic/predictive assessments? Appl Immunohistochem Mol Morphol 26: 760-768, 2017.
28. Korfias D, Contis J, Frangou-Plemenou M, Gennatas K, Kondis A and Vlachodimitropoulos D: Stem cells in ductal breast cancer: Immunohistochemical expression of CD44, CD24, CD133, and ALDH-1 markers in 104 cases. Eur J Gynaecol Oncol 41: 36-41, 2020.
29. Bamodu OA, Chung CC, Pisanic TR II and Wu ATH: The intricate interplay between cancer stem cells and cell-of-origin of cancer: Implications for therapeutic strategies. Front Oncol 14: 1404628, 2024.
30. Mengistu BA, Tsegaw T, Demessie Y, Getnet K, Bitew AB, Kinde MZ, Beirhun AM, Mebratu AS, Mekasha YT, Feleke MG and Fenta MD: Comprehensive review of drug resistance in mammalian cancer stem cells: Implications for cancer therapy. Cancer Cell Int 24: 406, 2024.
31. Park SY, Choi JH and Nam JS: Targeting cancer stem cells in triple-negative breast cancer. Cancers (Basel) 11: 965, 2019.
32. Murillo LL, Sugden CJ, Ozsvari B, Moftakhar Z, Hassan GS, Sotgia F and Lisanti MP: $ALDH^{High}$ breast cancer stem cells exhibit a mesenchymal-senescent hybrid phenotype, with elevated metabolic and migratory activities. Cells 13: 2059, 2024.
33. Ali R, Samman N, Al Zahrani H, Nehdi A, Rahman S, Khan AL, Al Balwi M, Alriyees LA, Alzaid M, Al Askar A and Boudjelal M: Isolation and characterization of a new naturally immortalized human breast carcinoma cell line, KAIMRC1. BMC Cancer 17: 803, 2017.
34. Ambrosio MR, Mosca G, Migliaccio T, Liguoro D, Nele G, Schonauer F, D'Andrea F, Liotti F, Prevete N, Melillo RM, *et al*: Glucose enhances pro-tumorigenic functions of mammary adipose-derived mesenchymal stromal/stem cells on breast cancer cell lines. Cancers (Basel) 14: 5421, 2022.
35. Ayodeji SA, Bao B, Teslow EA, Polin LA, Dyson G, Bollig-Fischer A and Fehl C: Hyperglycemia and O-GlcNAc transferase activity drive a cancer stem cell pathway in triple-negative breast cancer. Cancer Cell Int 23: 102, 2023.
36. Júnior JPL, Brescansin CP, Santos-Weiss ICR, Welter M, Souza EM, Rego FGM, Picheth G and Alberton D: Serum fluorescent advanced glycation End (F-AGE) products in gestational diabetes patients. Arch Endocrinol Metab 61: 233-237, 2017.
37. Kato S, Matsumura T, Sugawa H and Nagai R: Correlation between serum advanced glycation end-products and vascular complications in patient with type 2 diabetes. Sci Rep 14: 18722, 2024.
38. Sharaf H, Matou-Nasri S, Wang Q, Rabhan Z, Al-Eidi H, Al Abdulrahman A and Ahmed N: Advanced glycation endproducts increase proliferation, migration and invasion of the breast cancer cell line MDA-MB-231. Biochim Biophys Acta 1852: 429-441, 2015.
39. Matou-Nasri S, Sharaf H, Wang Q, Almobadel N, Rabhan Z, Al-Eidi H, Yahya WB, Trivilegio T, Ali R, Al-Shanti N and Ahmed N: Biological impact of advanced glycation endproducts on estrogen receptor breast cancer cell line MDA-MB-231. Biochim Biophys Acta Mol Basis Dis 1863: 2808-2820, 2017.
40. Alanazi F, Alsaleh AA, Alamoudi MK, Alasiri A, Haymond A and Matou-Nasri S: Targeting p70S6K1 inhibits glycated albumin-induced triple-negative breast cancer cell invasion and overexpression of galectin-3, a potential prognostic marker in diabetic patients with invasive breast cancer. Biomedicines 13: 612, 2025.
41. Brix N, Samaga D, Hennel R, Gehr K, Zitzelsberger H and Lauber K: The clonogenic assay: Robustness of plating efficiency-based analysis is strongly compromised by cellular cooperation. Radiat Oncol 15: 248, 2020.
42. Maashi Y, Almutairi S, Aldawood M, Al-Eidi H, AlRoshody R, Alghamdi HA, Bahattab S, Alsaleh AA, Alkadi H, Alghamdi S, *et al*: In vitro oncogenic effects of glycated albumin in human colorectal cancer cell lines HT29 and SW620 revealing EpCAM and Galectin-3 upregulation in Type 2 diabetic colorectal cancer tissues as potential biomarkers. J Oncol Res Ther 9: 10227, 2024.
43. Karthikeyan SK, Chandrashekar DS, Sahai S, Shrestha S, Aneja R, Singh R, Kleer CG, Kumar S, Qin ZS, Nakshatri H, *et al*: MammOnc-DB, an integrative breast cancer data analysis platform for target discovery. NPJ Breast Cancer 11: 35, 2025.
44. Staaf J, Häkkinen J, Hegardt C, Saal LH, Kimbung S, Hedenfalk I, Lien T, Sørlie T, Naume B, Russnes H, *et al*: RNA sequencing-based single sample predictors of molecular subtype and risk of recurrence for clinical assessment of early-stage breast cancer. NPJ Breast Cancer 8: 94, 2022.
45. Pereira B, Chin SF, Rueda OM, Vollan HK, Provenzano E, Bardwell HA, Pugh M, Jones L, Russell R, Sammut SJ, *et al*: The somatic mutation profiles of 2,433 breast cancers refines their genomic and transcriptomic landscapes. Nat Commun 7: 11479, 2016.
46. Cerami E, Gao J, Dogrusoz U, Gross BE, Sumer SO, Aksoy BA, Jacobsen A, Byrne CJ, Heuer ML, Larsson E, *et al*: The cBio cancer genomics portal: An open platform for exploring multidimensional cancer genomics data. Cancer Dicov 2: 401-404, 2012.
47. Gao J, Aksoy BA, Dogrusoz U, Dresdner G, Gross B, Sumer SO, Sun Y, Jacobsen A, Sinha R, Larsson E, *et al*: Integrative analysis of complex cancer genomics and clinical profiles using the cBioPortal. Sci Signal 2: pl1, 2013.
48. De Bruijn I, Kundra R, Mastrogiacomo B, Tran TN, Sikina L, Mazor T, Li X, Ochoa A, Zhao G, Lai B, *et al*: Analysis and visualization of longitudinal genomic and clinical data from the AACR project GENIE Biopharma collaborative in cBioPortal. Cancer Res 83: 3861-3867, 2023.
49. Rueda OM, Sammut SJ, Seoane JA, Chin SF, Caswell-Jin JL, Callari M, Batra R, Pereira B, Bruna A, Ali HR, *et al*: Dynamics of breast-cancer relapse reveal late-recurring ER-positive genomic subgroups. Nature 567: 399-404, 2019.
50. Curtis C, Shah SP, Chin SF, Turashvili G, Rueda OM, Dunning MJ, Speed D, Lynch AG, Samarajiwa S, Yuan Y, *et al*: The genomic and transcriptomic architecture of 2,000 breast tumours reveals novel subgroup. Nature 486: 346-352, 2012.
51. Panigrahi G, Candia J, Dorsey TH, Tang W, Ohara Y, Byun JS, Minas TZ, Zhang A, Ajao A, Cellini A, *et al*: Diabetes-associated breast cancer is molecularly distinct and shows a DNA damage repair deficiency. JCI Insight 8: e170105, 2023.
52. Wang S, Ma L, Wang Z, He H, Chen H, Duan Z, Li Y, Si Q, Chuang TH, Chen C, *et al*: Lactate dehydrogenase-A (LDH-A) preserves cancer stemness and recruitment of tumor-associated macrophages to promote breast cancer progression. Front Oncol 11: 654452, 2021.

53. Park YMM, Bookwalter DB, O'Brien KM, Jackson CL, Weinberg CR and Sandler DP: A prospective study of type 2 diabetes, metformin use, and risk of breast cancer. Ann Oncol 32: 351-359, 2021.
54. Zhang F, de Haan-Du J, Sidorenkov G, Landman GWD, Jalving M, Zhang Q and de Bock GH: Type 2 diabetes mellitus and clinicopathological tumor characteristics in women diagnosed with breast cancer: A systematic review and meta-analysis. Cancers (Basel) 13: 4992, 2021.
55. Abdelaty WR: Outcome of management of invasive lobular carcinoma in comparison to invasive ductal carcinoma. Al-Azhar Int Med J 5: 26, 2024.
56. Xiong JY, Wang JM, Zhao XL, Yang C, Jiang XS, Chen YM, Chen CQ and Li ZY: Glycated albumin as a biomarker for diagnosis of diabetes mellitus: A systematic review and meta-analysis. World J Clin Cases 9: 9520-9534, 2021.
57. Chiavarina B, Nokin MJ, Durieux F, Bianchi E, Turtoi A, Peulen O, Peixoto P, Irigaray P, Uchida K, Belpomme D, *et al*: Triple negative tumors accumulate significantly less methylglyoxal specific adducts than other human breast cancer subtypes. Oncotarget 5: 5472-5482, 2014.
58. Altundag-Erdogan Ö, Çetinkaya H, Öteyaka MÖ and Çelebi-Slatik B: Targeting MDA-MB-231 cancer stem cells with temsirolimus in 3D collagen/PGA/NA2SiO3-based bone model. Macromol Mater Engineer 310: 2400360, 2025.
59. Gomez-Salazar MA, Wang Y, Thottappillil N, Hardy RW, Alexandre M, Höller F, Martin N, Gonzalez-Galofre ZN, Stefancova D, Medici D, *et al*: Aldehyde dehydrogenase, a marker of normal and malignant stem cells, typifies mesenchymal progenitors in perivascular niches. Stem Cells Transl Med 12: 474-484, 2023.
60. Li B, Tian J, Zhang F, Wu C, Li Z, Wang D, Zhuang J, Chen S, Song W, Tang Y, *et al*: Self-assembled aldehyde dehydrogenase-activatable nano-prodrug for cancer stem cell-enriched tumor detection and treatment. Nat Commun 16: 9417, 2024.
61. Altshuler A, Wickstrom SA and Shalom-Feuerstein R: Spotlighting adult stem cells: Advances, pitfall, and challenges. Trends Cell Biol 33: 477-494, 2023.
62. Alvarez-Elizondo MB and Weihs D: Breast cancer stem cells: Mechanobiology reveals highly invasive cancer cell subpopulations. Cell Mol Life Sci 79: 134, 2022.
63. Ouyang M, Gui Y, Li N and Zhao L: Prognostic model based on tumor stemness genes for triple-negative breast cancer. Sci Rep 14: 30855, 2024.
64. Li X, Zhang Y, Gong J, Liu W, Zhao H, Xue H, Ren Z, Bao J and Lin Z: Development of a breast cancer invasion score to predict tumor aggressiveness and prognosis via PI3K/AKT/mTOR pathway analysis. Cell Death Disc 11: 157, 2025.
65. Nayak A, Warrier NM and Kumar P: Cancer stem cells and the tumor microenvironment: Targeting the critical crosstalk through nanocarrier system. Stem Cell Rev Rep 18: 2209-2233, 2022.
66. Chu X, Tian W, Ning J, Xiao G, Zhou Y, Wang Z, Zhai Z, Tanzhu G, Yang J and Zhou R: Cancer stem cells: Advances in knowledge and implications for cancer therapy. Signal Transduct Target Ther 9: 170, 2024.
67. Lee KJ, Yoo JW, Kim YK, Choi JH, Ha TY and Gil M: Advanced glycation end products promote triple negative breast cancer cells via ERK and NF-kB pathway. Biochem Biophys Res Commun 495: 2195-2201, 2018.
68. Khoo SH, Wu PR, Yeh KT, Hsu SL and Wu CH: Biological and clinical significance of the AGE-RAGE axis in the aggressiveness and prognosis of prostate cancer. J Food Drug Anal 31: 664-682, 2023.
69. Azizian-Farsani F, Abedpoor N, Sheikhha MH, Gure AO, Nasr-Esfahani MH and Ghaedi K: Receptor for advanced glycation end products acts as a fuel to colorectal cancer development. Front Oncol 10: 552283, 2020.
70. Nam HK, Jeong SR, Pyo MC, Ha SK, Nam MH and Lee KW: Methylglyoxal-derived advanced glycation end products (AGE4) promote cell proliferation and survival in renal cell carcinoma cells through the RAGE/Akt/ERK signaling pathways. Biol Pharm Bull 44: 1697-1706, 2021.
71. Galassi C, Manic G, Estellar M, Galluzzi L and Vitale I: Epigenetic regulation of cancer stemness. Sign Transduct Target Ther 10: 243, 2025.
72. Lee H, Kim B, Park J, Park S, Yoo G, Yum S, Kang W, Lee JM, Youn H and Youn B: Cancer stem cells: Landscape, challenges and emerging therapeutic innovations. Sign Transduct Target Ther 10: 248, 2025.
73. Khanh VC, Fukushige M, Moriguchi K, Yamashita T, Osaka M, Hiramatsu Y and Ohneda O: Type 2 diabetes mellitus induced paracrine effects on breast cancer metastasis through extracellular vesicles from human mesenchymal stem cells. Stem Cells Dev 29: 1382-1394, 2020.
74. Chang YH, Ngo NH, Vuong CK, Yamashita T, Osaka M, Hiramatsu Y and Ohneda O: Type 2 diabetes mellitus promotes the differentiation of adipose-derived mesenchymal stem cells into cancer-associated fibroblasts, induced by breast cancer cells. Stem Cells Dev 31: 659-671, 2022.
75. Viedma-rodríguez R, Martínez-Hernández MG, Martínez-Torres DI and Baiza-Gutman A: Epithelial mesenchymal transition and progression of breast cancer promoted by diabetes mellitus in mice are associated with increased expression of glycolytic and proteolytic enzymes. Horm Cancer 11: 170-181, 2020.
76. Baek KH, Choi J and Pei CZ: Cellular functions of OCT-3/4 regulated by ubiquitination in proliferating cells. Cancers (Basel) 12: 663, 2020.
77. Zhao FQ, Misra Y, Li DB, Wadsworth MP, Krag D, Weaver D, Tessitore J, Li DW, Zhang G, Tian Q and Buss K: Differential expression of Oct3/4 in human breast cancer and normal tissues. Int J Oncol 52: 2069-2078, 2018.
78. Shu S, Li Z, Liu L, Ying X, Zhang Y, Wang T, Zhou X, Jiang P and Lv W: HPV16 E6-activated OCT4 promotes cervical cancer progression by suppressing p53 expression via co-repressor NCOR1. Front Oncol 12: 900856, 2022.
79. Sun L, Liu T, Zhang S, Guo K and Liu Y: Oct4 induces EMT through LEF1/b-catenin dependent WNT signaling pathway in hepatocellular carcinoma. Oncol Lett 13: 2599-2606, 2017.
80. Berr AL, Wiese K, Dos Santos G, Koch CM, Anekalla KR, Kidd M, Davis JM, Cheng Y, Hu YS and Ridge KM: Vimentin is required for tumor progression and metastasis in a mouse model of non-small cell lung cancer. Oncogene 42: 2074-2087, 2023.
81. Pearson GW: Control of invasion by epithelial-to-mesenchymal transition programs during metastasis. J Clin Med 8: 646, 2019.
82. Yamashita N, Tokunaga E, Kitao Y, Taketani K, Akiyoshi S, Okada S, Aishima S, Morita M and Maehara Y: Vimentin as a prognostic factor for triple-negative breast cancer. J Cancer Res Clin Oncol 139: 739-746, 2013.
83. Chen Z, Fang Z and Ma J: Regulatory mechanisms and clinical significance of vimentin in breast cancer. Biomed Pharmacother 133: 111068, 2021.
84. Ahmadpour F, Igder S, Moghadam ARE, Moradipoodeh B, Sepahdar A, Mokarram P, Fallahi J and Mohammadzadeh G: Metformin as a potential therapeutic agent in breast cancer: Targeting miR-125a methylation and epigenetic regulation. Int J Mol Cell Med 13: 272-285, 2024.